Study on the Roles of BILL-cadherin/Cadherin-17 in the B Lymphocyte Differentiation and Antibody Response

A Dissertation Submitted to the Graduate School of Life and Environmental Sciences,
the University of Tsukuba in Partial Fulfillment of the Requirements
for the Degree of Doctor of Philosophy in Science
(Doctoral Program in Functional Biosciences)

Shuichi FUNAKOSHI

Table of Contents

Abbreviations

BEC: blood endothelial cell

BSA: bovine serum albumin

CDH17: cadherin-17

CGG: chicken gamma globulin

FRC: fibroblastic reticular cell

GC: germinal center

KO: knock-out

LEC: lymphatic endothelial cell

LLPC: long-lived plasma cell

MBC: memory B cell

MZ: marginal zone

PC: plasma cell

WT: wild-type

Abstract

Memory B cells (MBCs) and long-lived plasma cells (LLPCs) are responsible for immunological “memory”, which can last for many years. The long-term survival niche for LLPCs in the bone marrow is well characterized; however, the corresponding niche for MBCs is unclear. BILL-cadherin/cadherin-17 (CDH17) is the only member of the cadherin superfamily that is expressed on mouse B lymphocytes in a spatiotemporally regulated manner. Here, I show that half of all MBCs regain expression of CDH17 during the later stage of development. The maintenance of high affinity antigen-specific serum antibodies was impaired in $CDH17^{-/-}$ mice and the number of antigen-specific MBCs was reduced as compared to wild-type (WT) mice. Also, specific responses to secondary antigens were ablated in $CDH17^{-/-}$ mice, whereas primary antibody responses were the same as those in WT mice. Cell cycle analysis revealed a decline in the proliferation of $CDH17^{-}$ MBCs as compared to $CDH17^{+}$ MBCs. In addition, I identified a subpopulation of splenic stromal cells, MAdCAM-1^{+} blood endothelial cells (BEC), which was $CDH17^{+}$. Taken together, these results suggest that CDH17 plays a role in the long-term survival of MBCs, presumably via an "MBC niche" comprising, at least in part, BEC in the spleen.

General Introduction

BILL-cadherin/cadherin-17 (CDH17) is a cell adhesion molecule that belongs to the cadherin superfamily, a large group (more than 100 members) of cell adhesion molecules with properties similar to those of integrins and selectins. Cadherins are Ca^{2+}-dependent adhesion molecules characterized by their unique extracellular domains, which primarily comprise multiple cadherin-repeats (Figure 1). Cadherins primarily mediate homotypic (cell to cell) adhesion; therefore, they play important roles in intercellular recognition during embryogenesis and morphogenesis [Takeichi, 1995; Takeichi, 2007].

CDH17 contains seven cadherin domains and has no catenin-binding region within its cytoplasmic domain; the latter feature means that CDH17 is classified as a non-classical cadherin [Berndorff et al., 1994; Ohnishi et al., 2000]. CDH17 requires Ca^{2+} for homotypic adhesion [Ohnishi et al., 2000; Wendeler et al., 2007]; however, heterotypic adhesion to E-cadherin and $\alpha_2\beta_1$ integrin has been reported [Bartolome et al., 2014; Baumgartner et al., 2008]. In mice, CDH17 is expressed in the spleen, bone marrow, and intestine [Angres et al., 2001; Ohnishi et al., 2000], whereas in rats it is also expressed in the liver [Berndorff et al., 1994].

Immune system is an important defense mechanism to protect us from foreign organisms such as bacteria and viruses. It is composed by various cells, and they play specialized roles respectively. B cell is a lymphocyte that produces antibody, also known

as immunoglobulin, to bind with foreign pathogens then eliminates or neutralizes them. Because each antibody recognizes only one particular epitope and each B cell clone produces only one kind of antibody, it needs large numbers of B cell clone to eliminate various pathogens. To solve this problem, B cell recombines their antibody gene when they encountered the new pathogen. This is an essential function for the immune system. The B cells that obtained specialized antibody gene subsequently differentiate into either PCs (plasma cells) to produce antibody, or MBCs (memory B cells) to survive for long term in the body. MBCs can respond faster on the secondary exposure of pathogen and eliminate them more efficiently [Parkin and Cohen, 2001]. In addition, this system is the pivot of vaccination. Therefore, the long-term maintenance of MBCs is required for the effective protection and vaccination.

Here, I show that CDH17 plays an important role in the long-term survival of MBCs, thereby maintaining the capability for rapid antibody production during a secondary immune response. In addition, I found that a fraction of MAdCAM-1^{+} BEC may represent a candidate constituent of the MBC survival niche. Further elucidation of the molecular mechanisms underlying the role of CDH17 in MBC maintenance may make it possible to establish improved vaccination protocols.

Chapter 1

Functional Analyses of BILL-cadherin/Cadherin-17 Expressed on the Memory B Cell

Introduction

It was previously shown that precursor B cells express CDH17 during early development in the bone marrow [Ohnishi et al., 2005]. T cells, however, do not express CDH17 [Ohnishi et al., 2005; Ohnishi et al., 2000]. CDH17 is expressed during the pro-B/pre-B-I stages before being downregulated during the pre-B-II stage; it is then upregulated again on immature B cells [Ohnishi et al., 2000]. To elucidate the biological role of CDH17, CDH17-deficient ($CDH17^{-/-}$) mice were established previously [Ohnishi et al., 2005]. In $CDH17^{-/-}$ mice, exons which encode the trans-membrane region were disrupted by targeted gene replacement. Because CDH17 is type-1 trans-membrane protein, the deletion of these exons causes the loss of anchorage and hence abolishes its function. It was reported that CDH17-deficient mice have an increased number of pro-B cells and a reduced number of immature B cells, indicating that CDH17 plays a role(s) in early B cell development (i.e., during transition from the pro/pre-B-I stage to the pre-B-II stage) [Ohnishi et al., 2005]. Also, the size and the number of germinal centers (GC) in non-immunized $CDH17^{-/-}$ mice are reduced, and the antibody response to a T-independent antigen is decreased as compared to WT mice [Ohnishi et al., 2005]. These observations suggest that CDH17 might also play a role in late B cell development.

Here, I show that the expression of CDH17 was "spatiotemporally" regulated during

late B cell development. I compared T cell-dependent antigen-specific antibody responses to nitrophenylated chicken gammaglobulin (NP-CGG) in wild-type (WT) mice with those in CDH17$^{-/-}$ mice. The results showed that CDH17 contributes to the long-term survival of memory B cells.

Materials and Methods

Mice and ethics statements

CDH17$^{-/-}$ mice (CDH17 knock-out mice, BT262) were generated as previously described [Ohnishi et al., 2005]. The CDH17$^{-/-}$ mice were backcrossed onto a C57BL/6 background for ten generations. CDH17$^{+/+}$ and CDH17$^{-/-}$ homozygous littermates were used for all experiments. All mice were bred and maintained in a specific-pathogen-free (SPF) facility. All animal experiments were performed according to institutional guidelines and with the approval of the National Institute of Infectious Diseases Animal Care and Use Committee (Permit Number: 213045-2). Mice were housed under a 12 h light/dark cycle, and provided with food and water ad libitum. All efforts were made to minimize suffering. Mice were immunized intraperitoneally with antigen in a volume of less than 200 μL containing 50% Alum adjuvant. Blood samples were drawn from the tail vein and less than 100 μL was collected each time. Mice were euthanized by carbon dioxide inhalation and the spleens were explanted.

Antibodies and reagents

A rat monoclonal antibody (BD1B) against mouse CDH17 was raised as previously described [Ohnishi et al., 2000]. The following antibodies and reagents were purchased

from BD Pharmingen: PE/Cy7-anti-mouse IgM (catalog number, 552867; working dilution, 1:100), biotin-anti-mouse CD11a/integrin α_L (557365; 1:100), biotin-anti-mouse CD18/integrin β_2 (557439; 1:100), FITC-anti-mouse CD21 (553818; 1:100), FITC-anti-mouse Igλ (553434; 1:100), PE-anti-mouse CD23 (01235B; 1:50), APC-anti-mouse CD138 (558626; 1:100), PE-anti-mouse CD45R/B220 (01125B; 1:100), and PE-streptavidin (554061; 1:500). The following antibodies were purchased from eBioscience: eFluor 450-anti-mouse IgD (48-5993-80; 1:100), Alexa Fluor 488-anti-mouse/human GL7 (53-5902-80; 1:200), Pacific Blue-anti-mouse/human CD45R/B220 (57-0452-82; 1:100), and Alexa Fluor 700-anti-mouse CD38 (56-0381-82; 1:100). The following antibodies were purchased from BioLegend: PerCP/Cy5.5-anti-mouse IgG1 (406611; 1:100), PE-anti-mouse CD144/VE-cadherin (138009; 1:100), Alexa Fluor 647-anti-mouse CD80 (104717; 1:100), PE/Cy5-anti-mouse Gr-1 (108410; 1:100), PE/Cy5-anti-mouse TER-119 (116210; 1:100), PE/Cy5-anti-mouse CD3ε (100310; 1:100), APC/Cy7-anti-mouse/human CD45R/B220 (103224; 1:100), FITC-anti-mouse IgG1 (406606; 1:100), Alexa Fluor 700-anti-human CD19 (302225; 1:100), and FITC-anti-human CD27 (302805; 1:100). Pacific Blue-anti-BrdU (B35129; 1:100), Qdot 705-streptavidin (Q10163MP; 1:100), and O-phenylenediamine (002003) were purchased from Invitrogen. Alexa Fluor 488-anti-mouse CXCR3 (FAB1685G;

1:100) and Alexa Fluor 488-anti-mouse CCR6 (FAB590G; 1:100) were purchased from R&D Systems. The following antibody was obtained from Abcam: FITC-anti-mouse CD273 (ab59872; 1:100). Biotin-anti-mouse IgD (1120-08; 1:100), HRP-anti-mouse IgM (1020-05; 1:5000), and HRP-anti-mouse IgG1 (1144-05; 1:50000) were obtained from Southern Biotech. Alexa Fluor 430-streptavidin (S11237; 1:100) was obtained from Molecular Probes. The following reagents were purchased from Sigma-Aldrich: 7-AAD (A9400-1MG; 10 μg/mL) and 5-bromo-2'-deoxyuridine (BrdU; B5002-250MG). The following reagents were obtained from Biosearch Technologies: (4-hydroxy-3-nitro-phenyl)-acetyl $(NP)_{48}$-CGG, NP_4-BSA, and NP_{16}-BSA. Dispase (17105-041; 0.8 mg/mL) and collagenase IV (17104-019; 50 U/mL) were from Gibco. PE/Texas Red-streptavidin (IM3326, 1:100) was from Beckman Coulter. Tissue-Tek O.C.T. Compound (4583) was from Sakura. Finally, the following antibodies and reagents were generated in-house: biotin-BD1B, Alexa Fluor 647-BD1B, PE/Texas Red-BD1B, anti-mouse CD16-2 (2.4G2, 20 μg/mL), and NP_{44}-CGG. PE-(4-hydroxy-5-iodo-3-nitro-phenyl)-acetyl $(NIP)_{25}$ was a kind gift from Dr. Takahashi (Department of Immunology, National Institute of Infectious Diseases, Tokyo, Japan). The closely-related epitopes, NP and NIP, react with the same spectrum of specific antibodies [Bruggemann et al., 1986]. NIP is widely used for flow cytometry because it

has high affinity for NP-specific B cells. Therefore, NP was used in the ELISA because the number of NP-haptens on the CGG-carrier had to be controlled. NIP was used for flow cytometry.

Immunizations

For the primary antibody response experiments, 3- to 4-month-old $CDH17^{+/+}$ and $CDH17^{-/-}$ littermates were immunized intraperitoneally with 50 μg of NP_{48}-CGG precipitated with 100 μL of Imject Alum adjuvant (Thermo Scientific, 77161).

For the secondary antibody response experiments, 10- to 11-week-old $CDH17^{+/+}$ and $CDH17^{-/-}$ littermates were immunized intraperitoneally with 5 μg of NP_{44}-CGG precipitated with 100 μL of Imject Alum adjuvant. The mice were then boosted with an intraperitoneal injection of NP_{44}-CGG (2.5 μg) 50 weeks later.

ELISA

Flat-bottom 96-well plates (Immuno-MaxiSorp; Nunc 442404) were coated with 5 μg/mL of $NP_{1.6}$-BSA (to detect high affinity anti-NP antibodies) or with 5 μg/mL NP_4-BSA or NP_{16}-BSA (to detect total affinity anti-NP antibodies) and incubated at room temperature for 2 h or at 4°C overnight, followed by incubation with 1% BSA in

PBS/0.05% Tween 20 (Sigma, P-1379). Sera collected from immunized littermates were serially diluted, added to the plates, and incubated for 1 h at room temperature, followed by incubation with HRP-anti-mouse IgM or HRP-anti-mouse IgG1 antibodies. Hydrogen peroxide in citrate buffer and O-phenylenediamine were used as the chromogen. Optical density was measured at 490 nm. NP-specific IgM and IgG1 monoclonal antibodies (established in-house) were used as standards to calculate the relative antibody titers and affinities.

Flow cytometry

Mice were euthanized by CO_2 inhalation. Spleens were excised and spleen cell suspensions were prepared by mechanical disruption in staining buffer (Hank's Balanced Salt Solution (HBSS) containing 1% bovine serum albumin and 0.05% sodium azide), followed by filtering through a stainless steel mesh. To detect T1, T2, marginal zone (MZ), and mature B cells, cell suspensions were prepared from spleens isolated from $CDH17^{+/+}$ and $CDH17^{-/-}$ mice. Briefly, spleens were treated with 2.4G2 (20 μg/mL) for 30 min on ice to block Fcγ receptors and then stained with PE/Cy5-anti-Gr-1, PE/Cy5-anti-Ter-119, PE/Cy5-anti-CD3ε, APC/Cy7-anti-B220, eFluor 450-anti-mouse IgD, PE/Cy7-anti-mouse IgM, and Alexa Fluor 647-BD1B for 60 min on ice (working dilutions are provided in the

antibodies and reagents section). T1, T2, and MZ B cells were also stained with PE-anti-CD23 and FITC-anti-CD21. After washing well, the cells (5×10^6 cells/mL) were suspended in staining buffer containing 5 μg/mL propidium iodide (PI). About 1×10^6 cells were analyzed in a BD FACSAria III (BD Biosciences) and dead cells (PI^+) were excluded. This was the basic protocol for flow cytometry analysis and was used for all analyses described below.

To detect NP-specific GC B cells, cell suspensions were prepared from spleens on Day 12 post-immunization with NP-CGG, treated with 2.4G2 to block Fcγ receptors, and then stained with PE/Cy5-anti-Gr-1, PE/Cy5-anti-Ter-119, PE/Cy5-anti-CD3ε, APC/Cy7-anti-B220, eFluor 450-anti-mouse IgD, PE/Cy7-anti-mouse IgM, Alexa Fluor 700-anti-CD38, PE-NIP_{25}, Alexa Fluor 488-anti-GL7, and PE/Texas Red-BD1B. PI was added to exclude PI^+ dead cells.

To detect NP-specific plasma cells (PCs), littermates were immunized with NP-CGG, followed by a boost immunization on Day 196. Cell suspensions were isolated from spleens on Day 7 after the boost immunization, treated with 2.4G2 to block Fcγ receptors, and then stained with PE/Cy5-anti-Gr-1, PE/Cy5-anti-Ter-119, PE/Cy5-anti-CD3ε, Pacific Blue-anti-B220, APC-anti-CD138, PE-NIP_{25}, FITC-anti-Igλ biotin-BD1B, and Alexa Fluor 430-streptavidin. PI was added to exclude PI^+ dead cells.

To detect NP-specific MBCs, cell suspensions were isolated from the spleens of littermates immunized with NP-CGG, treated with 2.4G2 to block Fcγ receptors, and then stained with PE/Cy5-anti-Gr-1, PE/Cy5-anti-Ter-119, PE/Cy5-anti-CD3ε, APC/Cy7-anti-B220, eFluor 450-anti-mouse IgD, PE/Cy7-anti-mouse IgM, Alexa Fluor 700-anti-CD38, PE-NIP_{25}, FITC-anti-mouse IgG1, and Alexa Fluor 647-BD1B. PI was added to exclude PI^+ dead cells.

To detect surface markers on MBCs, cell suspensions were isolated from the spleens of littermates, treated with 2.4G2 to block Fcγ receptors, and then stained with PE/Cy5-anti-Gr-1, PE/Cy5-anti-Ter-119, PE/Cy5-anti-CD3ε, APC/Cy7-anti-B220, eFluor 450-anti-mouse IgD, PE/Cy7-anti-mouse IgM, Alexa Fluor 700-anti-CD38, PerCP/Cy5.5-anti-mouse IgG1, Qdot 705-streptavidin, Alexa Fluor 647-BD1B, Alexa Fluor 488-anti-mouse CXCR3, biotin-anti-mouse CD18, Alexa Fluor 488-anti-mouse CCR6, biotin-anti-mouse CD11a, biotin-BD1B, Alexa Fluor 647-anti-mouse CD80, FITC-anti-mouse CD273, and PE-anti-mouse CD144. PI was added to exclude PI^+ dead cells.

Cell cycle analysis

To examine the cell cycle status of $IgG1^+$ MBCs, $CDH17^{+/+}$ and $CDH17^{-/-}$ littermates

(17 ± 3-months-old) received an intraperitoneal injection of BrdU (1 mg) 1 h before sacrifice. Cell suspensions were isolated from the spleens, treated with 2.4G2 to block Fcγ receptors, and then stained with APC/Cy7-anti-B220, PE/Cy7-anti-mouse IgM, Alexa Fluor 700-anti-CD38, PE-NIP_{25}, FITC-anti-mouse IgG1, Alexa Fluor 647-BD1B, biotin-anti-mouse IgD, and PE/Texas Red-streptavidin. The cells were fixed with 1% paraformaldehyde/PBS at 0°C for 1 h and permeabilized with 0.05% NP-40/1% paraformaldehyde/PBS at 4°C overnight. Cells were then washed twice with 1% glycine/PBS and treated with DNase I solution (1 mg/mL DNase I, 1 mM $CaCl_2$, and 1 mM $MgCl_2$ in PBS) at 37°C for 10 min, followed by staining with Pacific Blue-anti-BrdU at room temperature for 45 min. Cells were suspended in 7AAD and the amount of DNA was measured by flow cytometry.

Statistical analysis

Microsoft Excel was used for statistical analysis. The error bars on the figures represent the standard deviation from the mean. Serum antibody titers, the net difference in serum antibody titers before and after the secondary immunization, the percentage of MBCs, and the MBC cell cycle indices were tested using the Mann-Whitney U-test. All other data were tested using Student's t-test. In all cases, differences were considered significant at

$p<0.05$ (*$p<0.05$, **$p<0.01$, and ***$p<0.001$).

Results

Differentiation-dependent regulation of CDH17 expression during late stages of B cell development

To investigate the possible roles of CDH17 in late B cell responses, I first analyzed the expression of CDH17 by various splenic B cell populations in WT and in CDH17$^{-/-}$ mice immunized with NP-CGG. Whereas transitional-1 B cells (T1 B; Lin$^-$B220$^+$IgD$^-$CD23$^-$CD21$^-$IgM$^+$) were CDH17$^-$, almost all transitional-2 B cells (T2 B; Lin$^-$B220$^+$IgD$^+$CD23$^+$CD21$^+$IgM$^+$) were CDH17$^+$. Marginal zone B cells (MZ B; Lin$^-$B220$^+$IgD$^-$CD23$^-$CD21$^+$IgM$^+$) were also CDH17$^+$ (Figure 2A). Both mature B cells (Lin$^-$B220$^+$IgD$^+$IgM$^-$) and antigen-specific PCs (Lin$^-$B220$^-$CD138$^+$IgG$^+$NIP$^+$) were CDH17$^-$ (Figure 2B, D). A small fraction of antigen-specific GC B cells (GC B; Lin$^-$B220$^+$GL7$^+$CD38$^{lo/-}$NIP$^+$) were CDH17^{+low} (Figure 2C). Interestingly, about half of antigen-specific MBCs (Lin$^-$B220$^+$IgD$^-$IgM$^-$CD38$^+$IgG1$^+$NIP$^+$) was CDH17$^+$ (Figure 2E). These data are consistent with DNA microarray data published in a previous report showing specific CDH17 expression by MBCs [Bhattacharya et al., 2007]. To further characterize the CDH17$^+$ and CDH17$^-$ MBCs, I next examined the expression of chemokine/cytokine receptors and other adhesion molecules (CXCR3, CCR6, integrin-β_2, integrin-α_L, VE-cadherin, CD80, and CD273) (Figure 3). Among these molecules,

CXCR3, integrin-α_L, integrin-β_2, CD80, and CD273 were expressed at slightly higher levels in $CDH17^+$ MBCs than in $CDH17^-$ MBCs.

These results show that the expression of CDH17 is tightly regulated during the late stages of B cell development: it is downregulated in T1 B cells, upregulated in T2 B cells, downregulated in mature B cells, and regained in MBCs during the GC reaction (Figure 2F, Figure 4). These observations raise the possibility that CDH17 might be involved in antibody affinity maturation and/or B cell memory.

The maintenance of serum antibody affinity is impaired in $CDH17^{-/-}$ mice

To elucidate the role of CDH17 in affinity maturation and MBC formation, I compared the antibody responses in WT and $CDH17^{-/-}$ mice. Mice were immunized with NP-CGG, and antigen-specific serum IgM (Figure 5A) and IgG1 (Figure 5B) antibody titers were measured. Antibody affinity for $NP_{1.6}$, NP_4, and NP_{16}-BSA was examined in an ELISA. There were no significant differences in the total NP-specific serum IgM and IgG1 titers between WT and $CDH17^{-/-}$ mice at 45 weeks after the primary immunization. However, when I examined WT and $CDH17^{-/-}$ mice for the presence of high affinity NP-specific serum antibodies, I found that the affinity of NP-specific serum IgM was lower in $CDH17^{-/-}$ mice than in WT mice at 4–6 weeks post-immunization (Figure 6A), and that

the affinity of IgG1 was lower in CDH17$^{-/-}$ mice from week 31 post-immunization (Figure 6B). Because there were no significant differences in the anti-NP_{16} total antibody titer between WT and CDH17$^{-/-}$ mice, the lower affinity of IgM and IgG1 in CDH17$^{-/-}$ mice must be due to a reduction in the high affinity anti-$NP_{1.6}$ and anti-NP_4 antibody titers. Since no significant differences were detected between WT and CDH17$^{-/-}$ mice during the early stages of immunization, the results also suggest that CDH17 becomes important during the later stages of an immune response, e.g., by promoting long-term maintenance of high affinity antigen-specific antibody titers.

The secondary antibody response is markedly impaired in CDH17$^{-/-}$ mice

High affinity antibody titers are thought to be maintained by MBCs and LLPCs. Because PCs are CDH17^{-} and about half of MBCs are CDH17^{+} (Figure 2), one possible explanation for the loss of high affinity antibodies could be impaired maintenance of high affinity-NP-specific MBCs in CDH17$^{-/-}$ mice. To test this hypothesis, I examined secondary antibody responses to NP-CGG. WT and CDH17$^{-/-}$ mice were boost immunized with NP-CGG in the absence of alum adjuvant at around 50 weeks post-priming. The increases in NP-specific serum antibody titers at Day 5 post-boost were then compared with those before the boost. I found that the NP-specific serum IgM and

IgG1 titers in WT mice increased markedly at Day 5 post-boosting. On the other hand, there was only a small increase in boosted CDH17$^{-/-}$ mice. The difference was most evident when changes in antibody titers were compared between individual mice. Antibody titers increased significantly in WT mice, whereas only a small increase or even a decrease was observed in individual CDH17$^{-/-}$ mice (Figure 7, Figure 8).

Because the NP-specific IgG1 titers at the time of the boost immunization were different between WT and CDH17$^{-/-}$ mice, I next compared the net difference in NP-specific serum IgG1 antibody titers before and after the secondary immunization (Figure 8). The differences in NP-specific serum IgM (excluding total NP_{16}-specific antibodies) and IgG1 titers were significantly higher in WT mice 5 days after the secondary immunization, but not in CDH17$^{-/-}$ mice. This bias was more evident for IgG1 antibodies (Figure 9). Because there were no significant differences in the NP-specific serum antibody titer between WT and CDH17$^{-/-}$ mice after the primary immunization, it appears that the defect in CDH17$^{-/-}$ mice is specific for the secondary antibody response.

In conclusion, these results showed that the secondary antibody response is functional, but impaired, in CDH17$^{-/-}$ mice, indicating that CDH17 affects the production of antigen-specific antibodies during the secondary immune response.

.

CDH17 contributes to the long-term maintenance of MBCs

Because CDH17$^{-/-}$ mice show an impaired secondary antibody response, I next examined whether antigen-specific MBCs were less common in CDH17$^{-/-}$ mice than in WT mice. WT and CDH17$^{-/-}$ mice were immunized with NP-CGG and changes in the percentage of NP-specific IgG1^{+} MBCs (Lin^{-}B220^{+}IgD^{-}IgM^{-}CD38^{+}IgG1^{+}NIP^{+}) were monitored by flow cytometry over a long time period (Figure 10A). There was no significant difference in the percentage of NP-specific MBCs between WT and CDH17$^{-/-}$ mice during the first 2–6 weeks post-immunization (Figure 10B), indicating that the initial rate of MBC development is not affected by CDH17 deficiency. Moreover, the number of progenitor cells, including mature B cells, T1 cells, T2 cells, antigen-specific GC B cells, and the total number of IgG1^{+} MBCs, was almost the same in WT and CDH17$^{-/-}$ mice (Figure 11, Figure 12). However, the number of NP-specific MBCs in CDH17$^{-/-}$ mice was significantly reduced (to about one-third of that in WT mice) after longer periods of time (50–67 weeks) post-immunization (Figure 10B). These results indicate that CDH17 plays an important role in the long-term maintenance of antigen-specific MBCs, which becomes clear after 50 weeks post-antigen exposure.

The "*in vivo*" proliferation of CDH17^{-} IgG1^{+} MBCs is significantly retarded

To elucidate the role of CDH17 in the long-term maintenance of MBCs, I next examined the influence of CDH17-deficiency on the rate of cell cycle entry, i.e., cell proliferation. Because the number of antigen-specific $IgG1^+$ MBCs was very small at 50 weeks post-primary immunization, I performed cell cycle analyses to examine switched $IgG1^+$ MBCs rather than antigen-specific $IgG1^+$ MBCs. WT and $CDH17^{-/-}$ mice (17 ± 3-months-old) were injected intraperitoneally with BrdU and sacrificed 1 h later. The cell cycle status of switched $IgG1^+$ MBCs ($B220^+IgD^-IgM^-CD38^+IgG1^+$) was then examined by flow cytometry (Figure 13, Figure 14). I analyzed the cell cycle status of switched $IgG1^+$ MBCs in $CDH17^+$ and $CDH17^-$ populations separately, and found that $CDH17^-$ $IgG1^+$ MBCs from WT mice showed the same cell cycle distribution as those from $CDH17^{-/-}$ mice. On the other hand, the cell cycle progression of $CDH17^+$ switched $IgG1^+$ MBCs was higher in WT mice (Figure 14B). These results suggest that CDH17 plays a role in the long-term maintenance of MBCs by increasing the rate at which MBCs enter the cell cycle.

Discussion

It was shown that almost half of MBCs express CDH17. I examined the expression of chemokine/cytokine receptors and other adhesion molecules (which are reported to be expressed on MBCs) on $CDH17^+$ and $CDH17^-$ MBCs [Bhattacharya et al., 2007; Tomayko et al., 2010]: CXCR3, CCR6, integrin-β_2, integrin-α_L, VE-cadherin, CD80, and CD273 (Figure 3). Of these, CXCR3, integrin-α_L, integrin-β_2, CD80, and CD273 were expressed at slightly higher levels on $CDH17^+$ MBCs than on $CDH17^-$ MBCs. Integrin-$\alpha_L\beta_2$ (LFA-1) is involved in B cell localization to the MZ [Lu and Cyster, 2002], suggesting that $CDH17^+$ MBCs are more likely to localize in the MZ than $CDH17^-$ MBCs. Also, MBCs are classified into five subsets according to their differential expression of CD273, CD73, and CD80; $CD80^{hi}$ and/or $CD273^{hi}$ cells are considered to be more "memory-like" [Tomayko et al., 2010]. The data presented herein suggest that $CD80^{hi}CD273^{hi}CDH17^+$ MBCs are more memory-like than $CDH17^-$ MBCs. Jones et al. reported that CXCR3 is expressed strongly in splenic MZ lymphoma [Jones et al., 2000], suggesting that it is involved in chemotaxis to the MZ. The fact that MBCs from $CDH17^{-/-}$ mice express levels of CXCR3 equivalent to those expressed by $CDH17^+$ MBCs implies that the upregulation of CDH17 occurs after the MBCs localize to the MZ.

CDH17-deficient mice showed a reduction in the titer of high affinity anti-NP

antibodies over time, without any obvious difference in the total antibody titer. Figure 5 and Figure 6 show that overall anti-NP_{16} IgG1 antibody titers changed: titers were almost equal in WT and CDH17$^{-/-}$ mice from Week 2 to Week 31, but were slightly lower in CDH17$^{-/-}$ mice at week 45; however, the difference was not statistically significant. The titers of high affinity IgG1 ($NP_{1.6}$ and NP_4) antibodies also changed: they were almost equal in WT and CDH17$^{-/-}$ mice at Weeks 2–6, but were slightly lower in CDH17$^{-/-}$ mice at Weeks 17–45. One possible explanation for this is that CDH17 is involved in the maintenance of MBCs but not in the formation of MBCs or PCs. I found that during the early phase of the antibody response (Weeks 2–6), there was no difference in antibody titers between WT and CDH17$^{-/-}$ mice because PCs developed equally well in both. During the later phase (Weeks 17–45), high affinity antibodies produced by PCs would be replenished; however, these antibodies would be different from those produced by maintained high affinity MBCs. The maintenance of high affinity MBCs was impaired in CDH17$^{-/-}$ mice, and the differentiation of PCs from MBCs decreased; therefore, the replenishment of high affinity antibodies also decreased. LLPCs, which developed during the early phase, continued to produce low affinity antibodies for a long time; thus the amount of antibodies produced by LLPCs in WT and CDH17$^{-/-}$ mice was the same because PCs do not express CDH17. Hence, after a long time post-antigen immunization,

the high affinity antibody ratios in $CDH17^{-/-}$ mice decreased and the total affinity antibody titer also decreased (slightly), even though the differences were not statistically significant.

I showed that the cell cycle turnover of $CDH17^{+}IgG1^{+}$ MBCs was faster than that of $CDH17^{-}$ MBCs. Recent reports examining $CDH17^{+}$ cancer cells reveal that cell cycle progression is slowed after CDH17 knockdown [Liu et al., 2009; Qiu et al., 2013]. The Wnt signaling pathway forms part of the cadherin signaling pathway [Conacci-Sorrell et al., 2002], which regulates the expression of cyclin D1. Immunoprecipitation experiments show that CDH17 associates with β-catenin, although CDH17 has no catenin-binding domain in its intracellular region [Bartolome et al., 2014]. These findings suggest that CDH17 accelerates cell cycle progression in $CDH17^{+}$ switched $IgG1^{+}$ MBCs via the Wnt signaling pathway.

Chapter 2

The Candidate Constituent of the BILL-cadherin/Cadherin-17-Mediated Memory B Cell Survival Niche

Introduction

Cells that are retained for long periods of time, such as hematopoietic stem cells, require a specialized niche for survival [Kunisaki et al., 2013; Morrison and Scadden, 2014]. In general, it is thought that the specific niche was constituted by stromal cells as one component and appropriate adhesion molecules are required for cells to reside within a specific niche. For example, memory $CD4^+$ T cells are resided at bone marrow by IL-7^+ stromal cells via integrin α_2 and MZ B cells are resided at MZ by ICAM-1^+ stromal cells via integrin $\alpha_L\beta_2$ respectively [Lu and Cyster, 2002; Tokoyoda et al., 2009]. Stromal cells are defined as non-hematopoietic cells that form a matrix. It was suggested that stromal cells have an important role for the regulation of immune response, such as the generation of lymphocytes, the tolerance induction, the response to antigen and the long-term maintenance of memory T cells [Tokoyoda et al., 2010]. MBCs might also require such a specialized survival niche to support their long-term maintenance; however, no such niche has been identified.

Several reports described that MBCs are localized at splenic MZ [Anderson et al., 2007; Dunn-Walters et al., 1995; Liu et al., 1988]. In addition, it was reported that CDH17 requires Ca^{2+} for homotypic adhesion [Ohnishi et al., 2000; Wendeler et al., 2007]. These facts indicate that some CDH17$^+$ stromal cell composes the survival niche for MBCs in

spleen and anchors MBCs via CDH17 homotypic adhesion.

Here, I identified a population of MAdCAM-1^{+} blood endothelial cells (BEC) that is CDH17^{+}. Taken together, these results suggest that CDH17^{+} BEC are a candidate for the elusive "MBC niche". The findings of the present study provide crucial clues that will improve our understanding of the mechanisms underlying long-term MBC survival.

Materials and Methods

Mice and ethics statements

See Chapter 1.

Antibodies and reagents

The following antibodies were purchased from BioLegend: APC/Cy7-anti-mouse CD45 (catalog number, 103116; working dilution, 1:100), Brilliant Violet 421 anti-mouse IgG1 (406615; 1:50), biotin-anti-mouse MAdCAM-1 (120705; 1:100), and Alexa Fluor 488-anti-mouse MAdCAM-1 (120707; 1:50). Alexa Fluor 488-anti-mouse Podoplanin (gp38) (53-5381-80; 1:100) was purchased from eBioscience. PE-anti-mouse CD31 (561073; 1:100) was purchased from BD Pharmingen. Qdot 655-streptavidin (Q10123MP; 1:100) was purchased from Invitrogen. Alexa Fluor 647-anti-mouse CD169 (MCA947A647; 1:100) was purchased from AbD Serotec. Other antibodies and reagents were described in Chapter 1.

Stromal cell analysis

To detect $CDH17^{+}$ stromal cells, spleen cells were fractionated according to the method of Fletcher et al. [Fletcher et al., 2011]. Briefly, spleens were pierced and treated with a

dispase (0.8 mg/mL)/collagenase IV (50 U/mL) enzyme mixture at 37°C for 20 min. The cell suspensions were generated by passage through a stainless sieve, then treated with 2.4G2 to block Fcγ receptors and stained with APC/Cy7-anti-mouse CD45, PE/Cy5-anti-Ter-119, Alexa Fluor 488-anti-mouse Podoplanin (gp38), PE-anti-mouse CD31, Alexa Fluor 647-BD1B, biotin-anti-mouse MAdCAM-1, and Qdot 705-streptavidin. PI was added to exclude PI^+ dead cells. Stained cells were then analyzed by flow cytometry as described above.

Confocal microscopy

Frozen spleen sections (6 μm thick) were treated with the Catalyzed Signal Amplification (CSA) System (Dako, K1500) to block endogenous peroxidase activity, followed by treatment with the Endogenous Biotin-Blocking Kit (Invitrogen, E21390) to block endogenous biotin and 2.4G2 to block Fcγ receptors. Sections were then stained with biotin-BD1B. After washing, the tissue sections were treated with a streptavidin biotin complex (CSA system) followed by the Individual Indirect Tyramide Reagent (PerkinElmer, SAT700001EA) to amplify the biotin-BD1B signal. Sections were then stained with Qdot 655-streptavidin, Alexa Fluor 647-anti-mouse CD169, Brilliant Violet 421 anti-mouse IgG1, and Alexa Fluor 488-anti-mouse MAdCAM-1. Immunostained

tissue sections were visualized under a Zeiss LSM710 confocal microscope. Data were analyzed using ZEN software.

Statistical analysis

Microsoft Excel was used for statistical analysis. The error bars on the figures represent the standard deviation from the mean. All data were tested using Student's t-test. Differences were considered significant at $p<0.05$.

Results

It is hypothesized that CDH17, expressed by splenic stromal cells, holds MBCs within a specific survival niche via homotypic adhesion. Several stromal cell subsets were defined in spleen. There are fibroblastic reticular cells (FRCs), follicular dendritic cells (FDCs), blood endothelial cells (BEC) and red pulp fibroblasts. Spleen can separate to two sections, such as white pulp and red pulp. The white pulp is a lymphoid compartment that consists of T cell zones and B cell follicles. FRC is localized at T cell zone and constructs FRC networks surrounding a central arteriole. FDC is localized at B cell follicle and constructs FDC networks too. BEC constructs several blood vessels, such as central arterioles, marginal sinus and red pulp sinus. MZ separates the white pulp and the red pulp [Mueller and Germain, 2009]. Some useful markers to identify stromal cell subsets were known. So I next examined the existence of $CDH17^{+}$ stromal cells as a possible constituent of the MBC survival niche by flow cytometry.

Mouse spleens were treated with dispase and collagenase IV, and the expression of CDH17 by various stromal cells was examined by flow cytometry (Figure 15A). By this procedure, stromal cells can be separated into four subpopulations, such as FRCs ($gp38^{+}CD31^{-}$), LECs ($gp38^{+}CD31^{+}$) and BECs ($gp38^{-}CD31^{+}$). I found that a fraction of MAdCAM-1^{+} BEC expressed significant levels of CDH17 (Figure 15B). However, it was

noticed that the endothelial cell surface was damaged by dispase/collagenase IV treatment. Although this may cause relatively high background signals, resulting in lower signal intensity for CDH17, I found that BEC expressed statistically significant levels of CDH17. In this context, I found that FRCs were also CDH17^{+}; however, in this case, the level of specific staining was not statistically significant due to the large standard deviation (Figure 15B). Thus, FRCs may be vulnerable to the harsh conditions caused by dispase/collagenase IV. Taken together, these results suggest that a CDH17-expressing subpopulation of MAdCAM-1^{+} BEC is a candidate constituent of the MBC survival niche.

In spleen, BECs can be attributed into several microarchitectures, such as central arterioles, marginal sinus and red pulp sinus. The results showed that MAdCAM-1^{+} BEC but not MAdCAM-1^{-} BEC expressed CDH17 (Figure 15B). MAdCAM-1 is expressed on cells lining the marginal sinuses, which partly overlap with the MOMA-1^{+} marginal zone [Kraal et al., 1995]. This observation indicates that a CDH17^{+} stromal cell is BEC that constructing marginal sinus at MZ. This speculation is consistent with the previous report by Liu et al. that MBC localized at MZ [Liu et al., 1988].

To confirm the existence of CDH17^{+}MAdCAM-1^{+} BEC in detail, I next performed histological experiments. It was shown that CDH17-expressing cells were localized in the

region overlapping these MOMA-1$^+$ cells and MAdCAM-1$^+$ cells; also, MAdCAM-1$^+$CDH17$^+$ cells were present in this region (although they were infrequent) (Figure 16). Overall, about 6% of cells in the MZ sinus (MAdCAM-1$^+$) were MAdCAM-1$^+$CDH17$^+$ BECs (Figure 17). Class-switched IgG1$^+$ B cells (B220$^+$IgM$^-$IgD$^-$IgG1$^+$) comprise about 0.01% of the splenic B220$^+$ B cell population, and about 70% of IgG1$^+$ B cells show a CD38$^+$ MBC phenotype (B220$^+$IgG1$^+$IgM$^-$IgD$^-$CD38$^+$). It is not easy to identify MBCs in the spleen by histology; however, small numbers of IgG1$^+$ B cells were consistently observed in association with white pulp, red pulp, or the MZ. Indeed, the number of IgG1$^+$ B cells found in the MZ was associated with cells those expressing MAdCAM-1 and CDH17 (Figure 16). The memory-like IgG1$^+$ B cells associated with MAdCAM-1$^+$CDH17$^+$ BEC were CDH17$^+$ (Figure 16, bottom panel), suggesting that CDH17 mediates adhesion. The number of IgG1$^+$ cells associated with the MZ area was significantly lower in CDH17$^{-/-}$ mice, whereas IgG1$^+$ cells on the red pulp or white pulp were not affected by CDH17-deficiency (Figure 18). These observations further support the idea that a CDH17-expressing subpopulation of MAdCAM-1$^+$ BEC located near marginal sinus constitutes a possible "MBC niche" in the spleen.

Discusion

It is thought that MBCs and memory T cells require a specific survival niche for long-term maintenance [Aiba et al., 2010; Dogan et al., 2009; Mueller and Germain, 2009; Tarlinton and Good-Jacobson, 2013]. The survival niches for memory $CD4^+$ T cells and LLPCs are well documented [Fairfax et al., 2008; Jelley-Gibbs et al., 2005; Tokoyoda et al., 2004]. Memory $CD4^+$ T cells and LLPCs are maintained by IL-7^+ stromal cells and by $CXCL12^+$ stromal cells, respectively, in the bone marrow. The number of maintained memory cells is limited by the available space within the survival niche. The methods used to create space for newly emerged memory cells within the survival niche have been reported [Xiang et al., 2007]. However, it is still unclear whether stromal cells are required for MBC survival and, if so, what kind of stromal cells were required [McHeyzer-Williams and Ahmed, 1999; Mueller and Germain, 2009; Tokoyoda et al., 2010]. Here, I showed that a fraction of MAdCAM-1^+ BEC express CDH17. According Kraal et al., MAdCAM-1^+ vascular cells in the spleen are marginal sinus endothelial cells [Kraal et al., 1995]. MBCs reside within the MZ in rodents and humans [Anderson et al., 2007; Dunn-Walters et al., 1995; Liu et al., 1988]. It was previously shown that the expression of CDH17 is especially high in the MZ [Ohnishi et al., 2000] (see also Figure 16). Thus, it was considered that the $CDH17^+$ BECs identified in the present study

comprise a fraction of the marginal sinus that offers an area suitable for CDH17-mediated homotypic-adhesion to MBC. Interestingly, recent studies show that endothelial cells within sinusoids comprise part of the stromal cell population that constitutes the hematopoietic stem cell niche [Kometani et al., 2013; Lu and Cyster, 2002; Mueller and Germain, 2009]. However, it cannot be excluded that other $CDH17^{+}$ sessile-type cells, such as FRCs or other as-yet-unidentified cells, contribute to the MBC survival niche. The frequency of MAdCAM-$1^{+}CDH17^{+}$ BECs in the MZ sinus (MAdCAM-1^{+}) was about 6% (Figure 17). It is not too low to support MBCs because a recent report shows that FRCs comprise about 30% of total stromal ($CD45^{-}$) cells and govern B cell homeostasis in mouse lymph nodes [Cremasco et al., 2014]. The memory-like $IgG1^{+}$ B cells shown in Figure 16 are $CDH17^{+}$. Collectively, these data suggest that a fraction of MAdCAM-1^{+} BEC, which expresses CDH17, comprises the MBC survival niche and that MBCs are anchored within this niche by homotypic adhesion mediated by CDH17 (Figure 19).

General Discussion

Here, I showed that CDH17, a cadherin molecule expressed differentially on B lymphocytes at different stages of development, plays a role in the long-term maintenance of antigen-specific MBCs. I found that the ability to sustain antigen-specific serum antibody titers and affinities over the long term was substantially impaired in CDH17-deficient mice. In addition, rapid antibody production during the early phase of the secondary response was markedly reduced in CDH17-deficient mice, indicating that CDH17 plays a role in the long-term preservation of MBC function, which assures rapid antibody production during a secondary immune response. The long-term existence of antigen-specific MBCs was also impaired in CDH17-deficient mice. I found that CDH17 participates in the maintenance of MBCs by regulating homeostatic cell cycle turnover. Moreover, I identified $CDH17^{+}$ splenic endothelial cells as a possible counterpart for CDH17-mediated homotypic adhesion of MBCs.

In humans, CDH17 is expressed in the fetal liver and gastrointestinal tract [Lee et al., 2010] but is downregulated in the adult liver and gastrointestinal tract; however, it is upregulated in gastric cancer, esophageal cancer, pancreatic cancer, and hepatocarcinoma [Liu et al., 2009; Su et al., 2008; Takamura et al., 2004]. CDH17 is also expressed on human B cell lines [Kim et al., 2006] and $CD19^{+}$ peripheral blood lymphocytes [Hutcheson et al., 2008], suggesting a role for CDH17 in human B cells. However, the

exact role of CDH17 in human MBCs remains unclear.

Recent reports on MBC localization in the mouse spleen identify the periphery of contractile GC as the region in which MBCs are maintained [Aiba et al., 2010; Anderson et al., 2007; Dogan et al., 2009]. As for the splenic microarchitecture around the GC and MZ, the inner layer of MOMA-1^+ metallophilic macrophages occasionally associates with the outer layer of GC in which CDH17 is also expressed. The difference between their experiments and ours is the timing of MBC examination: 8–25 weeks after the primary immunization in their case and after around 60 weeks in ours. The respective difference in the age of the MBCs would be reflected in the quality of the MBC population. In this context, it is noteworthy that I examined two populations of MBCs: $CDH17^+$ and $CDH17^-$. The current hypothesis is that these two types of MBC are generated by asymmetric cell division ("self-renewal" and "differentiation-oriented") on $CDH17^+$ BEC, as observed for hematopoietic stem cells [Knoblich, 2008]. It is speculated that the fate of $CDH17^+$ and $CDH17^-$ MBCs is as follows: whereas $CDH17^+$ MBCs remain within the $CDH17^+$ BEC niche and are maintained by homeostatic proliferation (which is presumably induced by catenin-mediated signaling via cell surface CDH17), $CDH17^-$ MBCs may leave the niche and differentiate into PCs, which partly replenish long-term antigen-specific antibodies. The differentiation of $CDH17^-$ MBCs into PCs requires antigen. It is speculated that, after

asymmetric cell division, CDH17$^-$ MBCs leave the MBC niche and circulate throughout the body until they encounter an antigen. If CDH17$^-$ MBCs do encounter an antigen, the cell is activated and differentiates into PCs to produce high affinity antibodies (if it does not encounter an antigen, the cell may die). It was reported that antigen-specific memory follicular T cells (Tfh) are in the draining regional lymph node [Fazilleau et al., 2007]. It is speculated that such cells may play a role in the activation of circulating CDH17$^-$ MBC. It would also be possible that circulating CDH17$^-$ MBCs are activated by polyclonal stimulation such as bystander T cell help and CpG DNA [Bernasconi et al., 2002]. In CDH17$^{-/-}$ mice, CDH17$^-$ MBCs localize out of the MBC niche in the spleen by adhering to molecules other than CDH17; hence, the cells lack a homeostatic proliferation signal.

Integrins $\alpha_L\beta_2$ and $\alpha_4\beta_1$ are required for MZ B cells to localize within the MZ [Lu and Cyster, 2002]. Cadherins are homotypic adhesion molecules that bind to the same species of cadherin molecule on a target cell, although heterotypic adhesion can also occur, such as adhesion between E-cadherin and integrins during T cell homing [Cepek et al., 1994; Karecla et al., 1995], and between CDH17 and E-cadherin [Baumgartner et al., 2008] or $\alpha_2\beta_1$ integrin [Bartolome et al., 2014]. Microarray experiments show that CDH17 is specifically expressed on MBCs in addition to α_4- and α_E-integrins [Bhattacharya et al., 2007]. The data presented herein strongly suggest that CDH17 is involved in MBC

homeostasis, probably through homotypic adhesion; however, it cannot be excluded heterotypic adhesion with integrins or other cadherins.

Based on these experimental results, I propose a possible model for long-term MBC maintenance (Figure 20). In this model, the initial rate of MBC development is the same in WT and CDH17$^{-/-}$ mice, resulting that the initial number of MBC is the same between WT and CDH17$^{-/-}$ mice. MBCs in WT mice are anchored at the MBC survival niche that composed by CDH17^{+}MAdCAM-1^{+} BEC lining the marginal sinuses via CDH17-mediated homotypic-adhesion. In contrast, MBCs in CDH17$^{-/-}$ mice cannot be localized at the niche, because it lacks the expression of CDH17. MBCs in WT mice can receive the survival signal from survival niche and show normal turnover rate. But MBCs in CDH17$^{-/-}$ mice show lower turnover rate because it cannot receive the survival signal. Therefore, the capability of MBCs maintenance and the secondary immune response are impaired at CDH17$^{-/-}$ mice. In conclusion, CDH17 is important for the long-term survival of MBC by enhancing the turnover rate and hence contributes to maintain the capability of the rapid antibody production in secondary response.

In conclusion, I showed that CDH17 plays an important role in the long-term survival of antigen-specific MBCs, thereby maintaining the capability for rapid antibody production during a secondary immune response. I found that a fraction of MAdCAM-1^{+}

BEC may represent a candidate constituent of the MBC survival niche. Further elucidation of the molecular mechanisms underlying the role of CDH17 in MBC maintenance may make it possible to establish improved vaccination protocols.

Acknowledgments

I gratefully appreciate Prof. Dr. Kazuo Ohnishi (National Institute of Infectious Diseases) for supervision of the course for doctoral degree. I am also thankful to Prof. Dr. Osamu Numata (Univ. of Tsukuba), Prof. Dr. Manabu Ato (National Institute of Infectious Diseases), Prof. Dr. Fritz Melchers (Max Plank Institute for Infection Biology), and Prof. Dr. Takeyuki Shimizu (Univ. of Kochi) for helpful advice and comments. I would like to express my gratitude to Ms. Sayuri Yamaguchi for valuable technical assistance.

References

Aiba Y, Kometani K, Hamadate M, Moriyama S, Sakaue-Sawano A, et al. (2010) Preferential localization of IgG memory B cells adjacent to contracted germinal centers. *Proc Natl Acad Sci U S A* **107**: 12192-12197.

Anderson SM, Tomayko MM, Ahuja A, Haberman AM, Shlomchik MJ (2007) New markers for murine memory B cells that define mutated and unmutated subsets. *J Exp Med* **204**: 2103-2114.

Angres B, Kim L, Jung R, Gessner R, Tauber R (2001) LI-cadherin gene expression during mouse intestinal development. *Dev Dyn* **221**: 182-193.

Bartolome RA, Barderas R, Torres S, Fernandez-Acenero MJ, Mendes M, et al. (2014) Cadherin-17 interacts with $\alpha_2\beta_1$ integrin to regulate cell proliferation and adhesion in colorectal cancer cells causing liver metastasis. *Oncogene* **33**: 1658-1669.

Baumgartner W, Wendeler MW, Weth A, Koob R, Drenckhahn D, et al. (2008) Heterotypic trans-interaction of LI- and E-cadherin and their localization in plasmalemmal microdomains. *J Mol Biol* **378**: 44-54.

Bernasconi NL, Traggiai E, Lanzavecchia A (2002) Maintenance of serological memory by polyclonal activation of human memory B cells. *Science* **298**: 2199-2202.

Berndorff D, Gessner R, Kreft B, Schnoy N, Lajous-Petter AM, et al. (1994) Liver-intestine cadherin: molecular cloning and characterization of a novel Ca^{2+}-dependent cell adhesion molecule expressed in liver and intestine. *J Cell Biol* **125**: 1353-1369.

Bhattacharya D, Cheah MT, Franco CB, Hosen N, Pin CL, et al. (2007) Transcriptional profiling of antigen-dependent murine B cell differentiation and memory formation. *J Immunol* **179**: 6808-6819.

Bruggemann M, Muller HJ, Burger C, Rajewsky K (1986) Idiotypic selection of an antibody mutant with changed hapten binding specificity, resulting from a point mutation in position 50 of the heavy chain. *EMBO J* **5**: 1561-1566.

Cepek KL, Shaw SK, Parker CM, Russell GJ, Morrow JS, et al. (1994) Adhesion between

epithelial cells and T lymphocytes mediated by E-cadherin and the $\alpha_E\beta_7$ integrin. *Nature* **372**: 190-193.

Conacci-Sorrell M, Zhurinsky J, Ben-Ze'ev A (2002) The cadherin-catenin adhesion system in signaling and cancer. *J Clin Invest* **109**: 987-991.

Cremasco V, Woodruff MC, Onder L, Cupovic J, Nieves-Bonilla JM, et al. (2014) B cell homeostasis and follicle confines are governed by fibroblastic reticular cells. *Nat Immunol* **15**: 973-981.

Dogan I, Bertocci B, Vilmont V, Delbos F, Megret J, et al. (2009) Multiple layers of B cell memory with different effector functions. *Nat Immunol* **10**: 1292-1299.

Dunn-Walters DK, Isaacson PG, Spencer J (1995) Analysis of mutations in immunoglobulin heavy chain variable region genes of microdissected marginal zone (MGZ) B cells suggests that the MGZ of human spleen is a reservoir of memory B cells. *J Exp Med* **182**: 559-566.

Fairfax KA, Kallies A, Nutt SL, Tarlinton DM (2008) Plasma cell development: from B-cell subsets to long-term survival niches. *Semin Immunol* **20**: 49-58.

Fazilleau N, Eisenbraun MD, Malherbe L, Ebright JN, Pogue-Caley RR, et al. (2007) Lymphoid reservoirs of antigen-specific memory T helper cells. *Nat Immunol* **8**: 753-761.

Fletcher AL, Malhotra D, Acton SE, Lukacs-Kornek V, Bellemare-Pelletier A, et al. (2011) Reproducible isolation of lymph node stromal cells reveals site-dependent differences in fibroblastic reticular cells. *Front Immunol* **2**: 35.

Hutcheson J, Scatizzi JC, Siddiqui AM, Haines GK, 3rd, Wu T, et al. (2008) Combined deficiency of proapoptotic regulators Bim and Fas results in the early onset of systemic autoimmunity. *Immunity* **28**: 206-217.

Jelley-Gibbs DM, Brown DM, Dibble JP, Haynes L, Eaton SM, et al. (2005) Unexpected prolonged presentation of influenza antigens promotes CD4 T cell memory generation. *J Exp Med* **202**: 697-706.

Jones D, Benjamin RJ, Shahsafaei A, Dorfman DM (2000) The chemokine receptor CXCR3 is expressed in a subset of B-cell lymphomas and is a marker of B-cell chronic lymphocytic leukemia. *Blood* **95**: 627-632.

Karecla PI, Bowden SJ, Green SJ, Kilshaw PJ (1995) Recognition of E-cadherin on epithelial cells by the mucosal T cell integrin $\alpha_{M290}\beta_7$ ($\alpha_E\beta_7$). *Eur J Immunol* **25**: 852-856.

Kim JW, Tchernyshyov I, Semenza GL, Dang CV (2006) HIF-1-mediated expression of pyruvate dehydrogenase kinase: a metabolic switch required for cellular adaptation to hypoxia. *Cell Metab* **3**: 177-185.

Knoblich JA (2008) Mechanisms of asymmetric stem cell division. *Cell* **132**: 583-597.

Kometani K, Nakagawa R, Shinnakasu R, Kaji T, Rybouchkin A, et al. (2013) Repression of the transcription factor Bach2 contributes to predisposition of IgG1 memory B cells toward plasma cell differentiation. *Immunity* **39**: 136-147.

Kraal G, Schornagel K, Streeter PR, Holzmann B, Butcher EC (1995) Expression of the

mucosal vascular addressin, MAdCAM-1, on sinus-lining cells in the spleen. *Am J Pathol* **147**: 763-771.

Kunisaki Y, Bruns I, Scheiermann C, Ahmed J, Pinho S, et al. (2013) Arteriolar niches maintain haematopoietic stem cell quiescence. *Nature* **502**: 637-643.

Lee NP, Poon RT, Shek FH, Ng IO, Luk JM (2010) Role of cadherin-17 in oncogenesis and potential therapeutic implications in hepatocellular carcinoma. *Biochim Biophys Acta* **1806**: 138-145.

Liu LX, Lee NP, Chan VW, Xue W, Zender L, et al. (2009) Targeting cadherin-17 inactivates Wnt signaling and inhibits tumor growth in liver carcinoma. *Hepatology* **50**: 1453-1463.

Liu YJ, Oldfield S, MacLennan IC (1988) Memory B cells in T cell-dependent antibody responses colonize the splenic marginal zones. *Eur J Immunol* **18**: 355-362.

Lu TT, Cyster JG (2002) Integrin-mediated long-term B cell retention in the splenic

marginal zone. *Science* **297**: 409-412.

McHeyzer-Williams MG, Ahmed R (1999) B cell memory and the long-lived plasma cell. *Curr Opin Immunol* **11**: 172-179.

Morrison SJ, Scadden DT (2014) The bone marrow niche for haematopoietic stem cells. *Nature* **505**: 327-334.

Mueller SN, Germain RN (2009) Stromal cell contributions to the homeostasis and functionality of the immune system. *Nat Rev Immunol* **9**: 618-629.

Ohnishi K, Melchers F, Shimizu T (2005) Lymphocyte-expressed BILL-cadherin/cadherin-17 contributes to the development of B cells at two stages. *Eur J Immunol* **35**: 957-963.

Ohnishi K, Shimizu T, Karasuyama H, Melchers F (2000) The identification of a nonclassical cadherin expressed during B cell development and its interaction with surrogate light chain. *J Biol Chem* **275**: 31134-31144.

Parkin J, Cohen B (2001) An overview of the immune system. *Lancet* **357**: 1777-1789.

Qiu HB, Zhang LY, Ren C, Zeng ZL, Wu WJ, et al. (2013) Targeting CDH17 suppresses tumor progression in gastric cancer by downregulating Wnt/β-catenin signaling. *PLoS One* **8**: e56959.

Su MC, Yuan RH, Lin CY, Jeng YM (2008) Cadherin-17 is a useful diagnostic marker for adenocarcinomas of the digestive system. *Mod Pathol* **21**: 1379-1386.

Takamura M, Ichida T, Matsuda Y, Kobayashi M, Yamagiwa S, et al. (2004) Reduced expression of liver-intestine cadherin is associated with progression and lymph node metastasis of human colorectal carcinoma. *Cancer Lett* **212**: 253-259.

Takeichi M (1995) Morphogenetic roles of classic cadherins. *Curr Opin Cell Biol* **7**: 619-627.

Takeichi M (2007) The cadherin superfamily in neuronal connections and interactions.

Nat Rev Neurosci **8**: 11-20.

Tarlinton D, Good-Jacobson K (2013) Diversity among memory B cells: origin, consequences, and utility. *Science* **341**: 1205-1211.

Tokoyoda K, Egawa T, Sugiyama T, Choi BI, Nagasawa T (2004) Cellular niches controlling B lymphocyte behavior within bone marrow during development. *Immunity* **20**: 707-718.

Tokoyoda K, Zehentmeier S, Hegazy AN, Albrecht I, Grun JR, et al. (2009) Professional memory $CD4^+$ T lymphocytes preferentially reside and rest in the bone marrow. *Immunity* **30**: 721-730.

Tokoyoda K, Hauser AE, Nakayama T, Radbruch A (2010) Organization of immunological memory by bone marrow stroma. *Nat Rev Immunol* **10**: 193-200.

Tomayko MM, Steinel NC, Anderson SM, Shlomchik MJ (2010) Cutting edge: Hierarchy of maturity of murine memory B cell subsets. *J Immunol* **185**: 7146-7150.

Wendeler MW, Drenckhahn D, Gessner R, Baumgartner W (2007) Intestinal LI-cadherin acts as a Ca^{2+}-dependent adhesion switch. *J Mol Biol* **370**: 220-230.

Xiang Z, Cutler AJ, Brownlie RJ, Fairfax K, Lawlor KE, et al. (2007) FcγRIIb controls bone marrow plasma cell persistence and apoptosis. *Nat Immunol* **8**: 419-429.

Figures

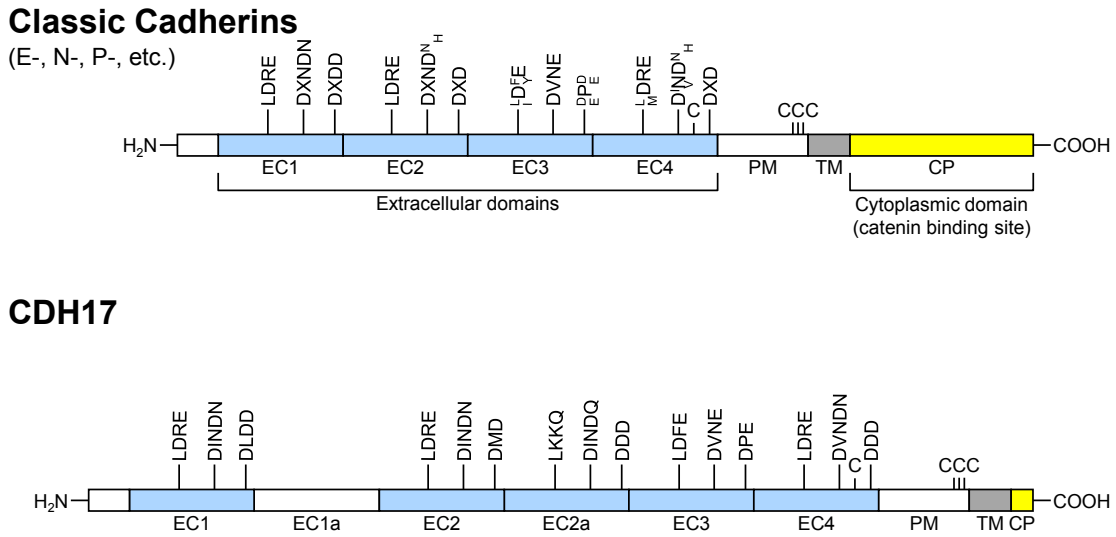

Figure 1. Domain structure of CDH17.

The organization of cadherin domains in CDH17 resembles non-classic rather than classic cadherins, since it lacks the ‘precursor segment’ and is composed of five cadherin domains and one pseudo-domain. The most striking difference from the classic cadherins is a lack of the "catenin-binding motif" in the cytoplasmic domain.

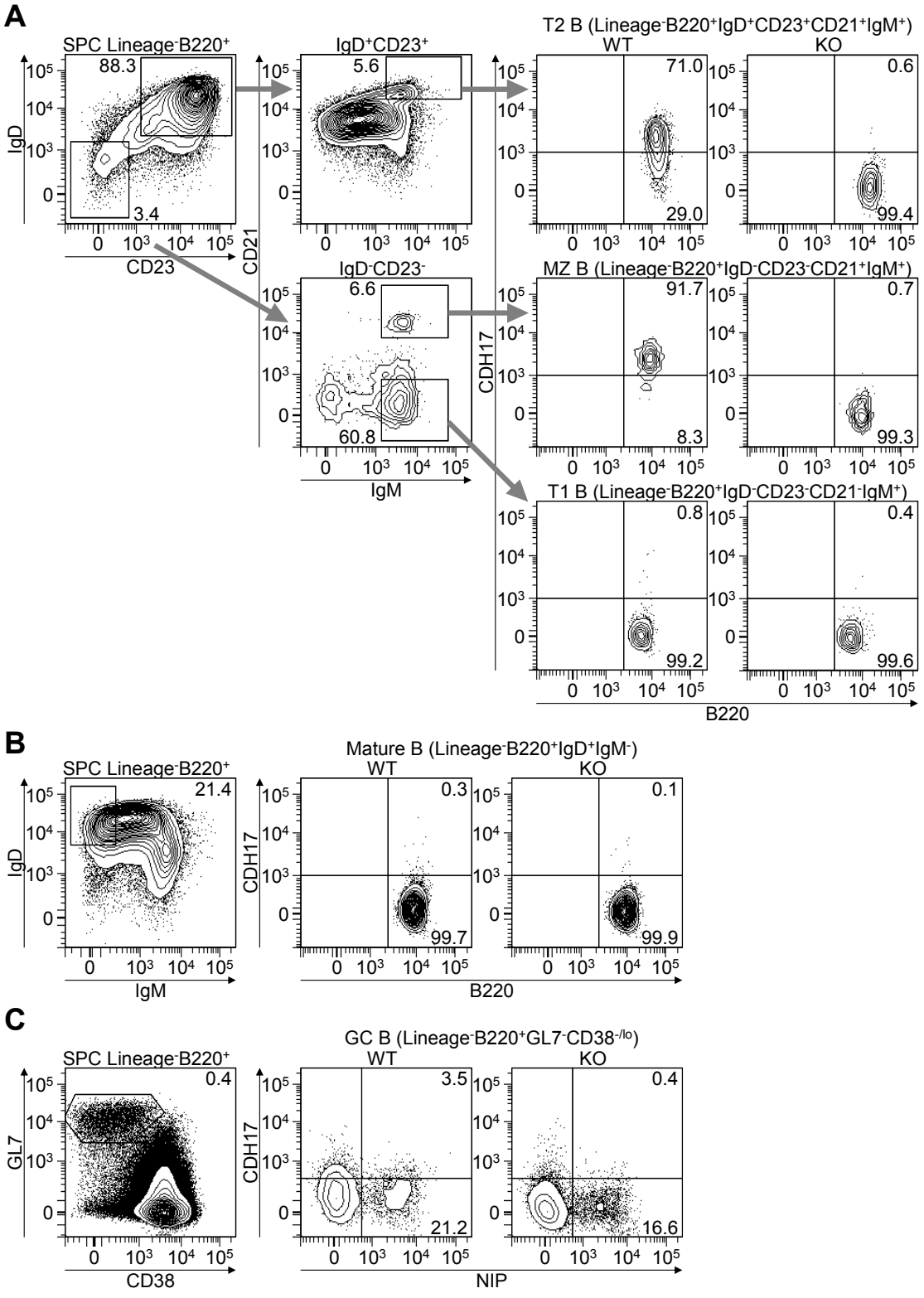
A
SPC Lineage-B220+
IgD
CD23
88.3
3.4
IgD+CD23+
CD21
5.6
IgD-CD23-
IgM
6.6
60.8
T2 B (Lineage-B220+IgD+CD23+CD21+IgM+)
WT
KO
71.0
29.0
0.6
99.4
MZ B (Lineage-B220+IgD-CD23-CD21+IgM+)
CDH17
91.7
8.3
0.7
99.3
T1 B (Lineage-B220+IgD-CD23-CD21-IgM+)
0.8
99.2
0.4
99.6
B220
B
SPC Lineage-B220+
IgD
IgM
21.4
Mature B (Lineage-B220+IgD+IgM-)
WT
KO
CDH17
0.3
99.7
0.1
99.9
B220
C
SPC Lineage-B220+
GL7
CD38
0.4
GC B (Lineage-B220+GL7-CD38-/lo)
WT
KO
CDH17
3.5
21.2
0.4
16.6
NIP

(Figure 2)

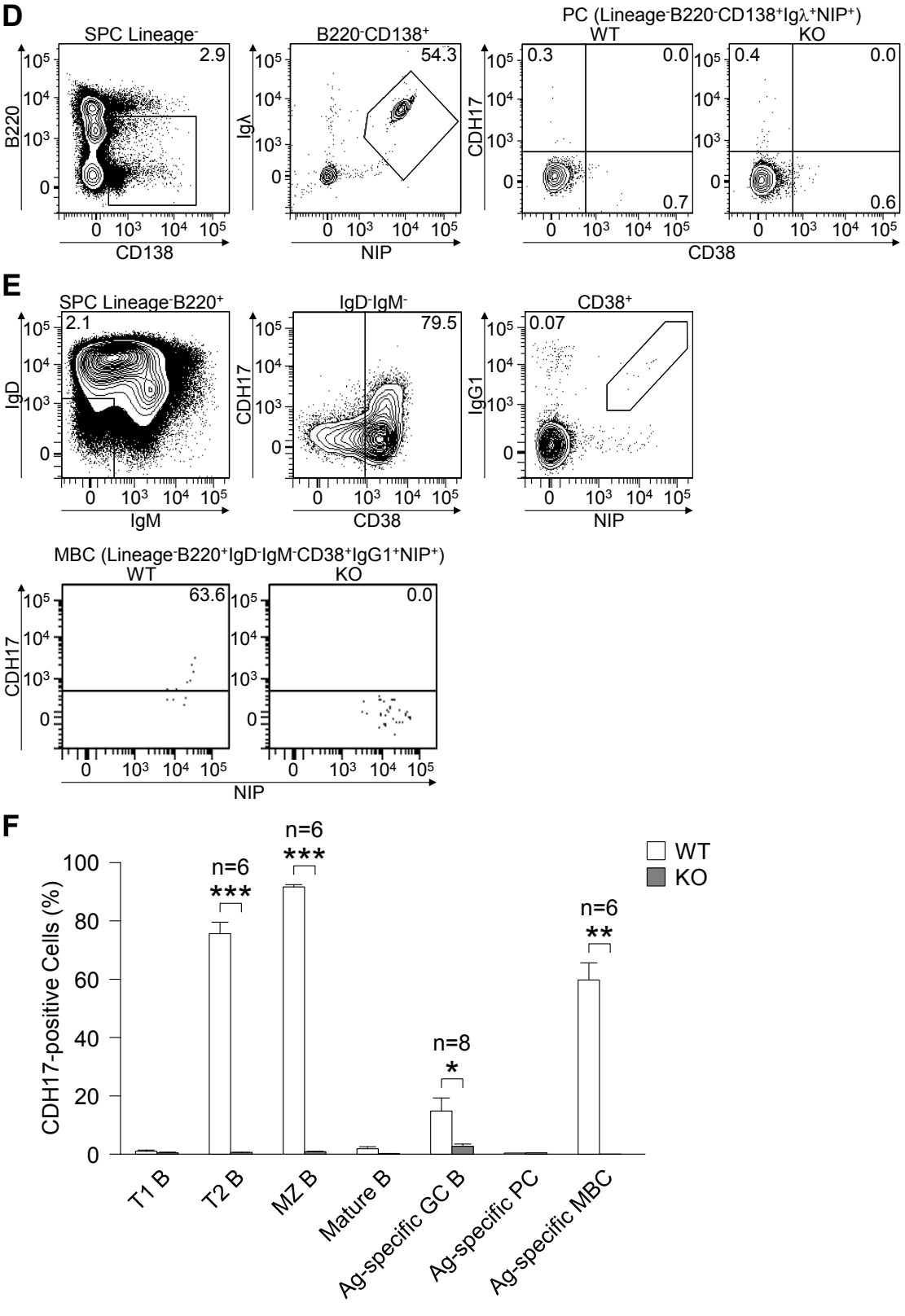
D
SPC Lineage-
2.9
B220
CD138
B220-CD138+
54.3
Igλ
NIP
PC (Lineage-B220-CD138+Igλ+NIP+)
WT
KO
0.3
0.0
0.7
0.4
0.0
0.6
CDH17
CD38
E
SPC Lineage-B220+
2.1
IgD
IgM
IgD-IgM-
79.5
CDH17
CD38
CD38+
0.07
IgG1
NIP
MBC (Lineage-B220+IgD-IgM-CD38+IgG1+NIP+)
WT
KO
63.6
0.0
CDH17
NIP
F
CDH17-positive Cells (%)
WT
KO
n=6
***
n=6
***
n=8
*
n=6
**
T1 B
T2 B
MZ B
Mature B
Ag-specific GC B
Ag-specific PC
Ag-specific MBC

(Figure 2)

Figure 2. The differentiation-dependent regulation of CDH17 expression during B cell development in spleen.

(A–E) Flow cytometry analysis of CDH17 expression on spleen cells and bone marrow cells isolated from wild-type (WT) and $CDH17^{-/-}$ (KO) mice. (A) T1 B cells ($Lin^-B220^+IgD^-CD23^-CD21^-IgM^+$), T2 B cells ($Lin^-B220^+IgD^+CD23^+CD21^+IgM^+$), and MZ B cells ($Lin^-B220^+IgD^-CD23^-CD21^+IgM^+$). (B) Mature B cells ($Lin^-B220^+IgD^+IgM^-$). (C) Antigen-specific GC B cells ($Lin^-B220^+GL7^+CD38^{low/-}NIP^+$). (D) Antigen-specific PCs ($Lin^-B220^-CD138^+Ig\lambda^+NIP^+$). (E) Antigen-specific MBCs ($Lin^-B220^+IgD^-IgM^-CD38^+IgG1^+NIP^+$). Numbers adjacent to the gates indicate the percentage (%) of cells in the respective parental gates. (F) Histogram showing the percentage of $CDH17^+$ cells within various B cell populations. The percentage of $CDH17^+$ cells relative to the total number of cells in the parental gates (indicated on the top of the corresponding flow cytometric contour plot) was calculated. In (C), the percentage of antigen-specific cells within the parental gates was calculated (n=2 (PCs), n=8 (GC B), n=6 (others); *P≤0.05, **P≤0.01, ***P≤0.001 (Student's t-test)).

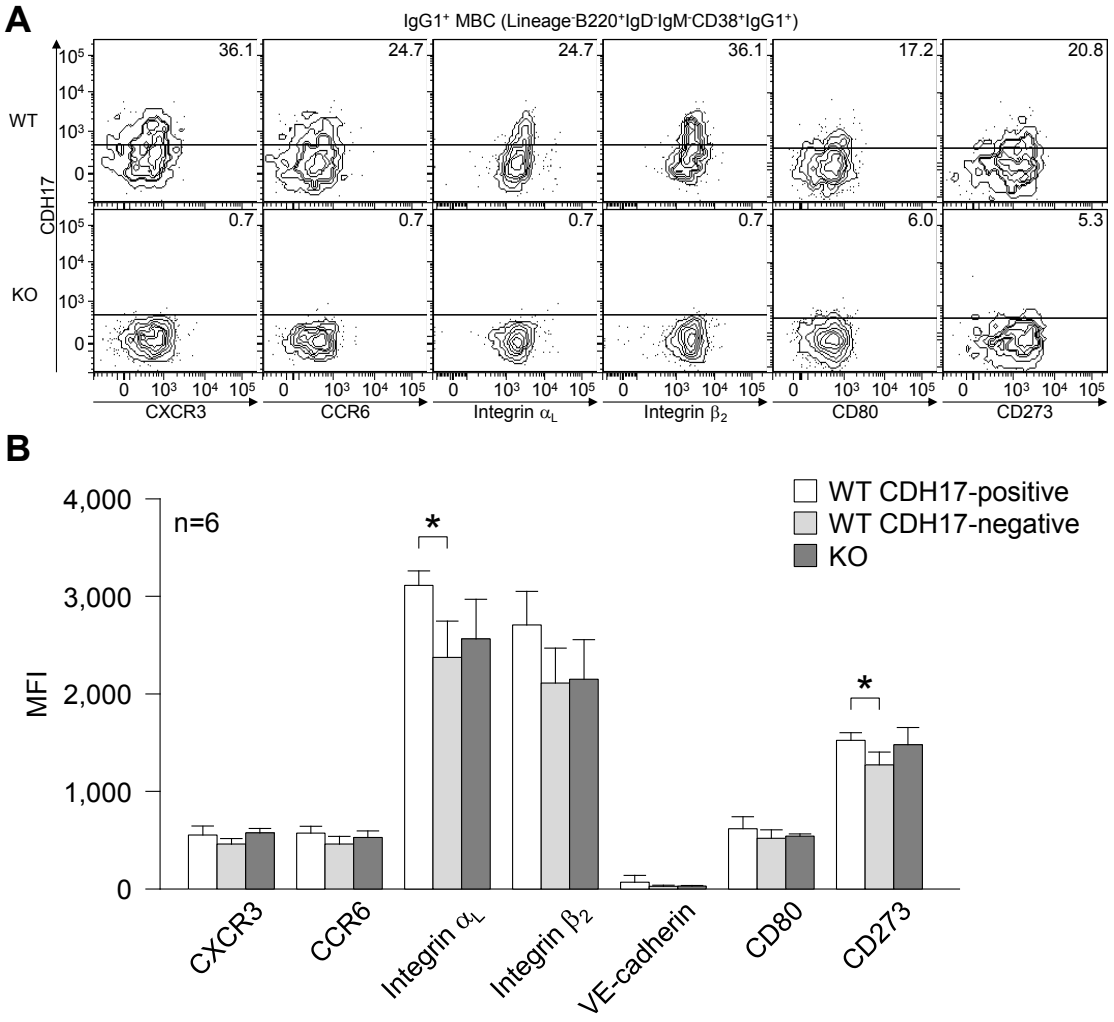

Figure 3. The expression of chemokine receptors, cell adhesion molecules, and co-stimulatory molecules by CDH17$^+$ and CDH17$^-$ MBCs.

(A) Expression profiles of two chemokine receptors, three adhesion molecules, and two co-stimulatory molecules on IgG1$^+$ MBCs (Lin$^-$B220$^+$IgD$^-$IgM$^-$CD38$^+$IgG1$^+$). Numbers represent the percentage (%) of CDH17$^+$ cells in the IgG1$^+$ MBC gate. (B) Histogram showing the mean fluorescence intensity (MFI) of each marker expressed on IgG1$^+$ MBCs (n=6; *P≤0.05 (Mann-Whitney U-test)).

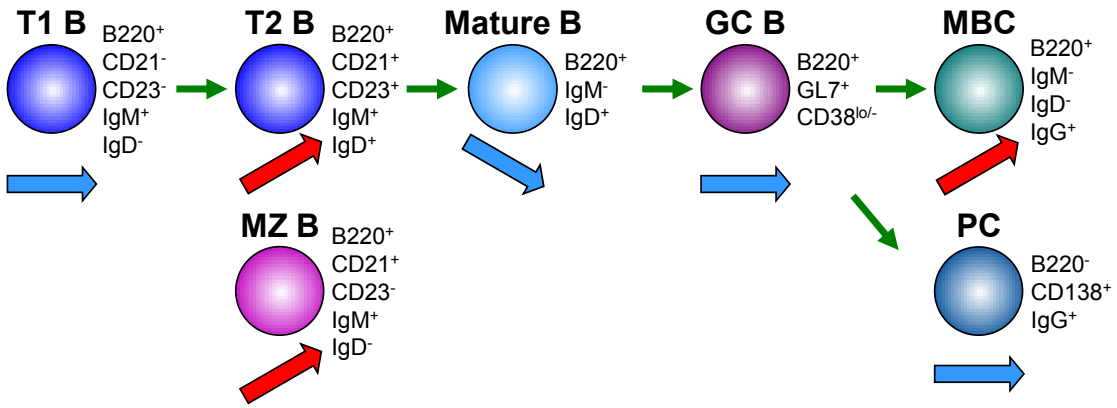

Figure 4. The "spatiotemporal" regulation of CDH17 expression during the B cell development in spleen.

The expression of CDH17 is downregulated in T1 B cells, upregulated in T2 B cells, downregulated in mature B cells, and regained in MBCs during the GC reaction. However, the expression of CDH17 in PCs remains negative. In addition, MZ B cells were CDH17-positive.

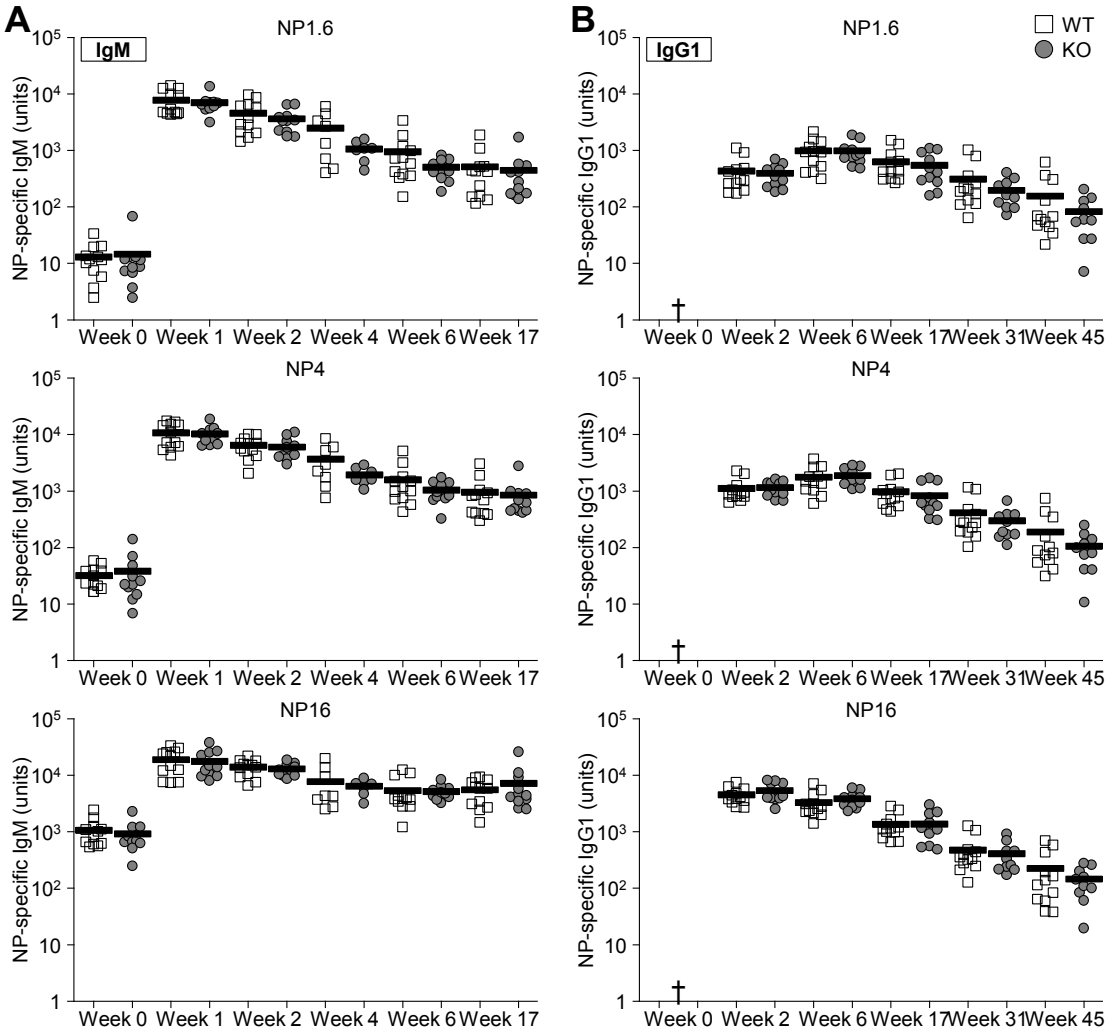

Figure 5. Ag-specific serum antibody titers in the primary immunization.

CDH17$^{-/-}$ (KO) mice and their WT littermates were immunized with NP-CGG in alum. The titers of serum IgM (A) and IgG1 (B) antibodies against NP-BSA were measured in an ELISA. Antibody titers are expressed in terms of units derived from a panel of reference monoclonal NP-specific antibodies. Each symbol represents an individual mouse. The mean values are represented by the bold lines. The titers of high affinity ($NP_{1.6}$), medium affinity (NP_4), and total affinity (NP_{16}) antibodies are shown. †Lower than 1 unit.

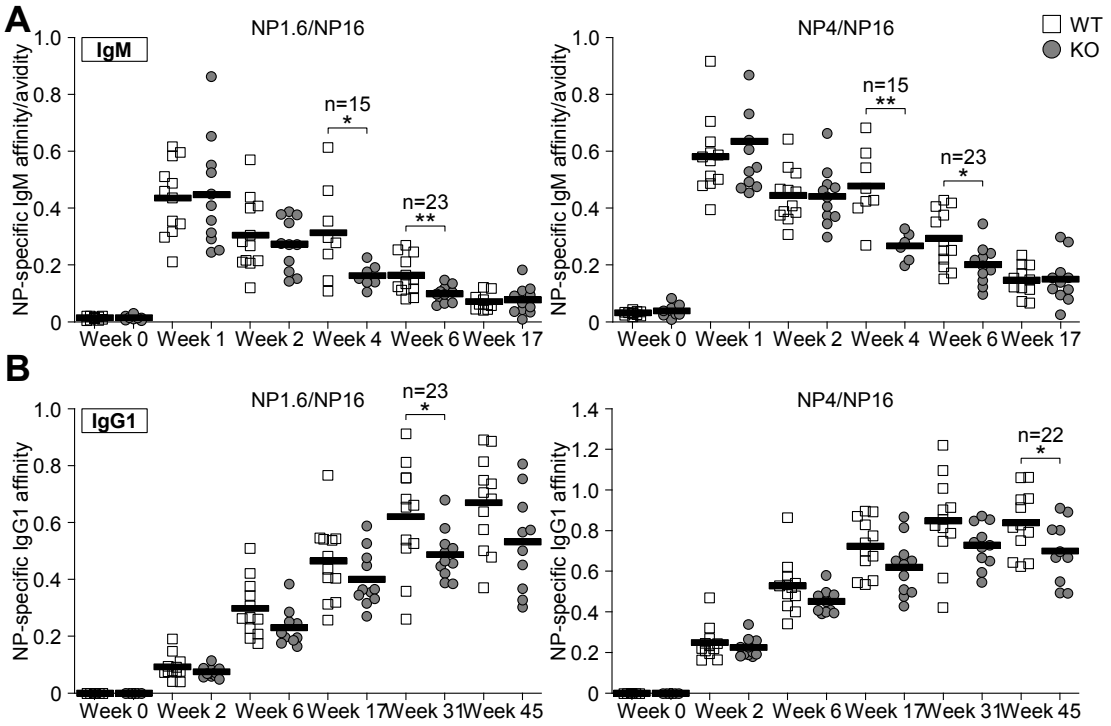

Figure 6. Ag-specific serum antibody affinities in the primary immunization.

Affinity ratios of serum IgM (A) or IgG1 (B) were calculated for high affinity ($NP_{1.6}/NP_{16}$) and medium affinity (NP_4/NP_{16}) antibodies using the data in Figure 5. Statistical significance was tested using Student's t-test (n=15 (Week 4); n=23 (other times); *P≤0.05, **P≤0.01).

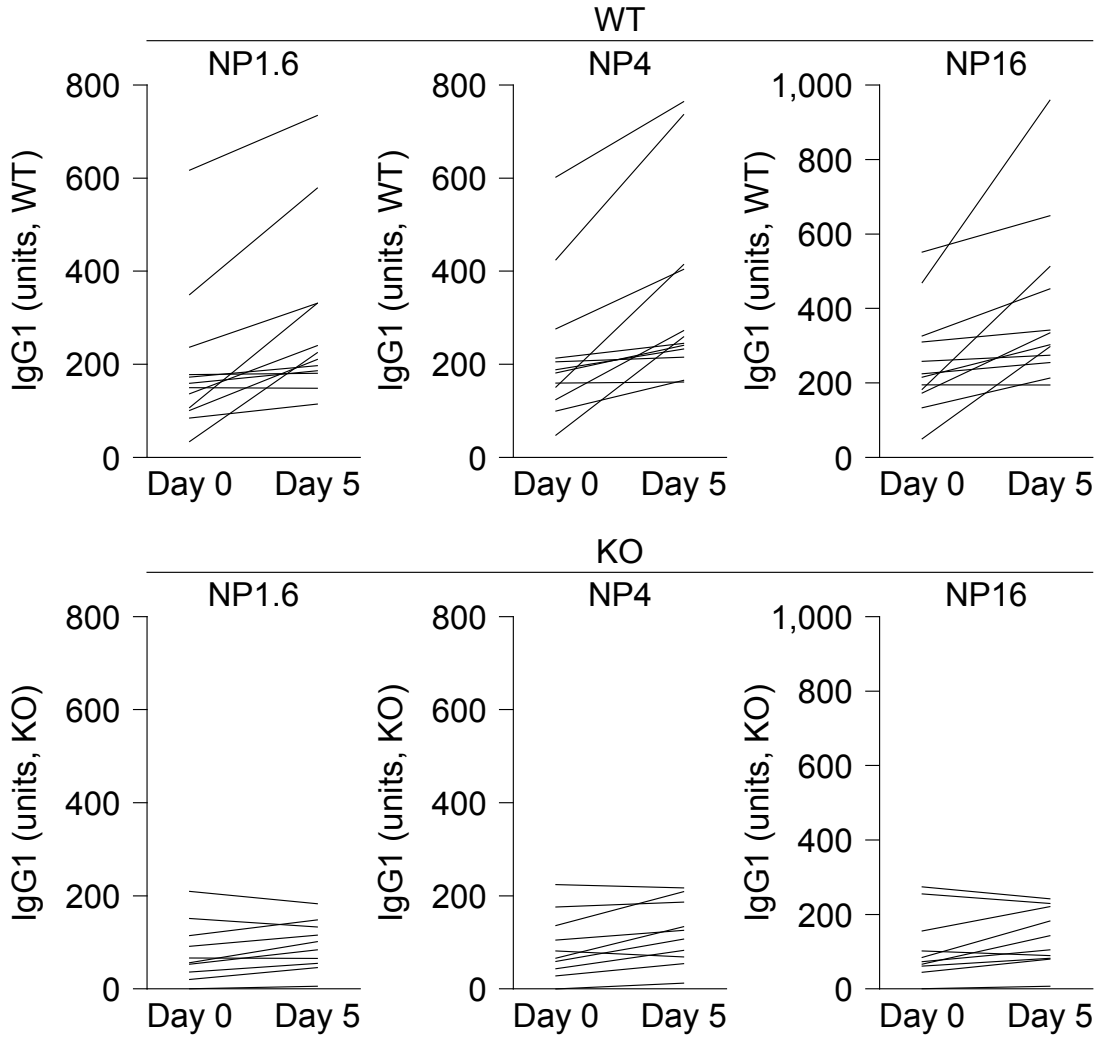

Figure 7. Ag-specific serum antibody titers in the secondary immunization.

CDH17$^{-/-}$ (KO) mice and their WT littermates received a primary immunization with NP-CGG in alum. Mice were boost immunized (without alum) 50 weeks later. Serum titers of anti-NP IgM and IgG1 antibodies were measured in an ELISA. Line graph showing the change in NP-specific serum IgG1 titer in individual mice (titers are expressed as described in the legend to Figure 5). The horizontal axis shows the day of blood sampling (Day 0 = the day of boost; Day 5 = 5 days post-boost). Each line represents an individual mouse.

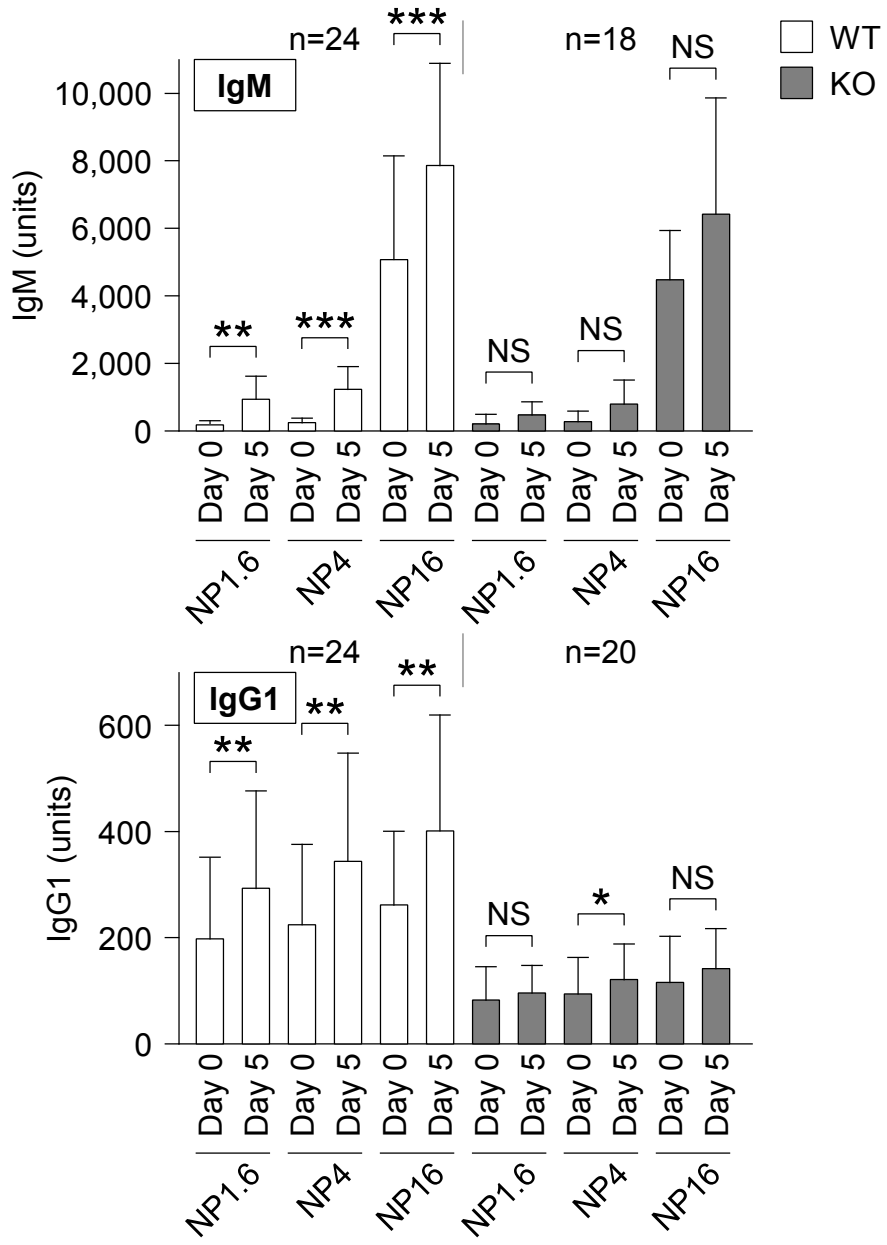

Figure 8. Comparison of serum antibody titers between pre- and post-boosting.

Histograms showing the average titers of NP-specific serum IgM (left) and IgG1 (right) calculated from the data shown in Figure 7. Statistical significance was calculated using a paired Student's t-test (n=24 (WT, IgM); n=18 (KO, IgM); n=24 (WT, IgG1); n=20 (KO, IgG1)). NS, not significant (P>0.05). *P≤0.05, **P≤0.01, ***P ≤0.001.

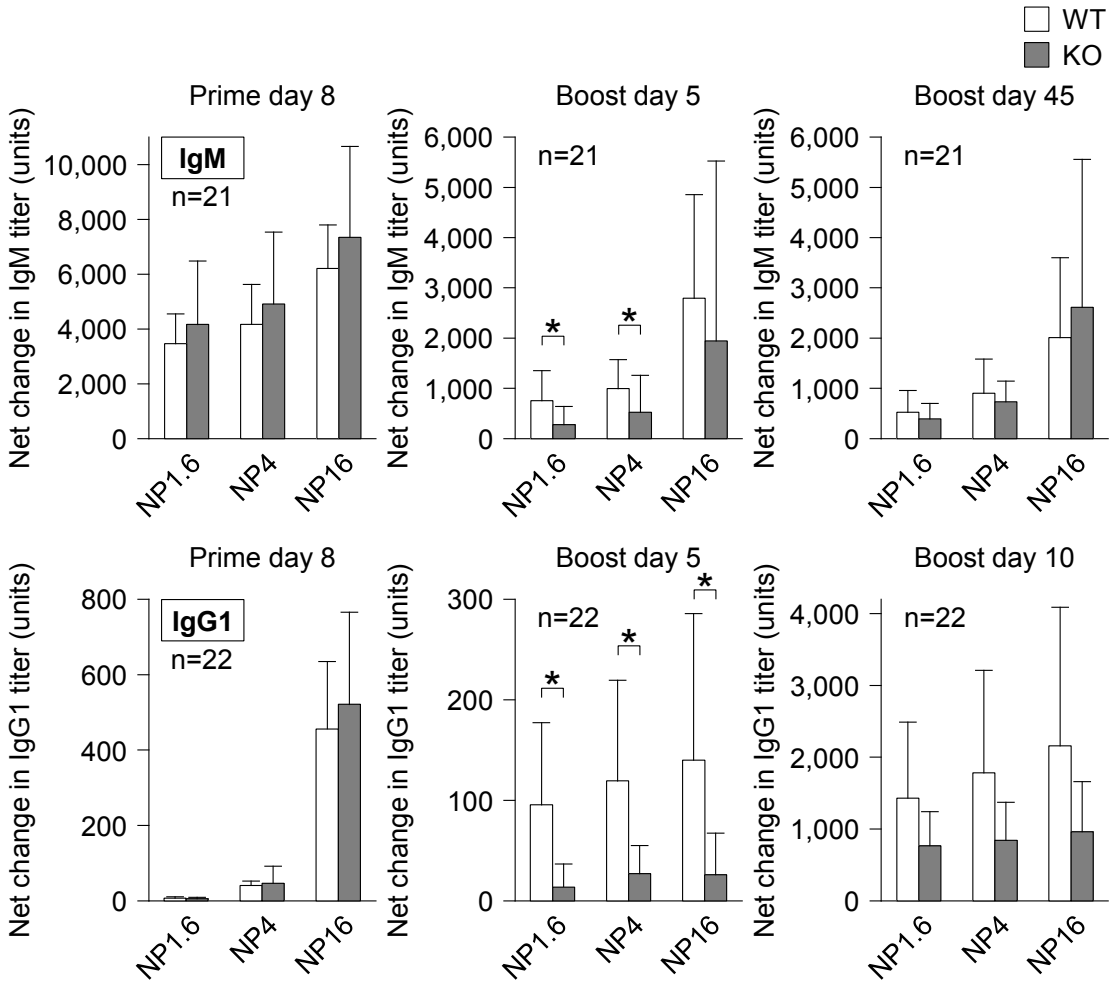

Figure 9. Comparison of serum antibody titers between WT and CDH17$^{-/-}$ mice.

The net increment of NP-specific serum IgM titers (top) and IgG1 titers (bottom) after the primary immunization (left) and boost immunization (middle, 5 days after the boost; right, 45 days after the boost) was calculated by subtracting the pre-immune (left) or pre-boost (middle and right) serum titers. Statistical significance was calculated using a Mann-Whitney U-test (n=21 (IgM); n=22 (IgG1)). *P≤0.05.

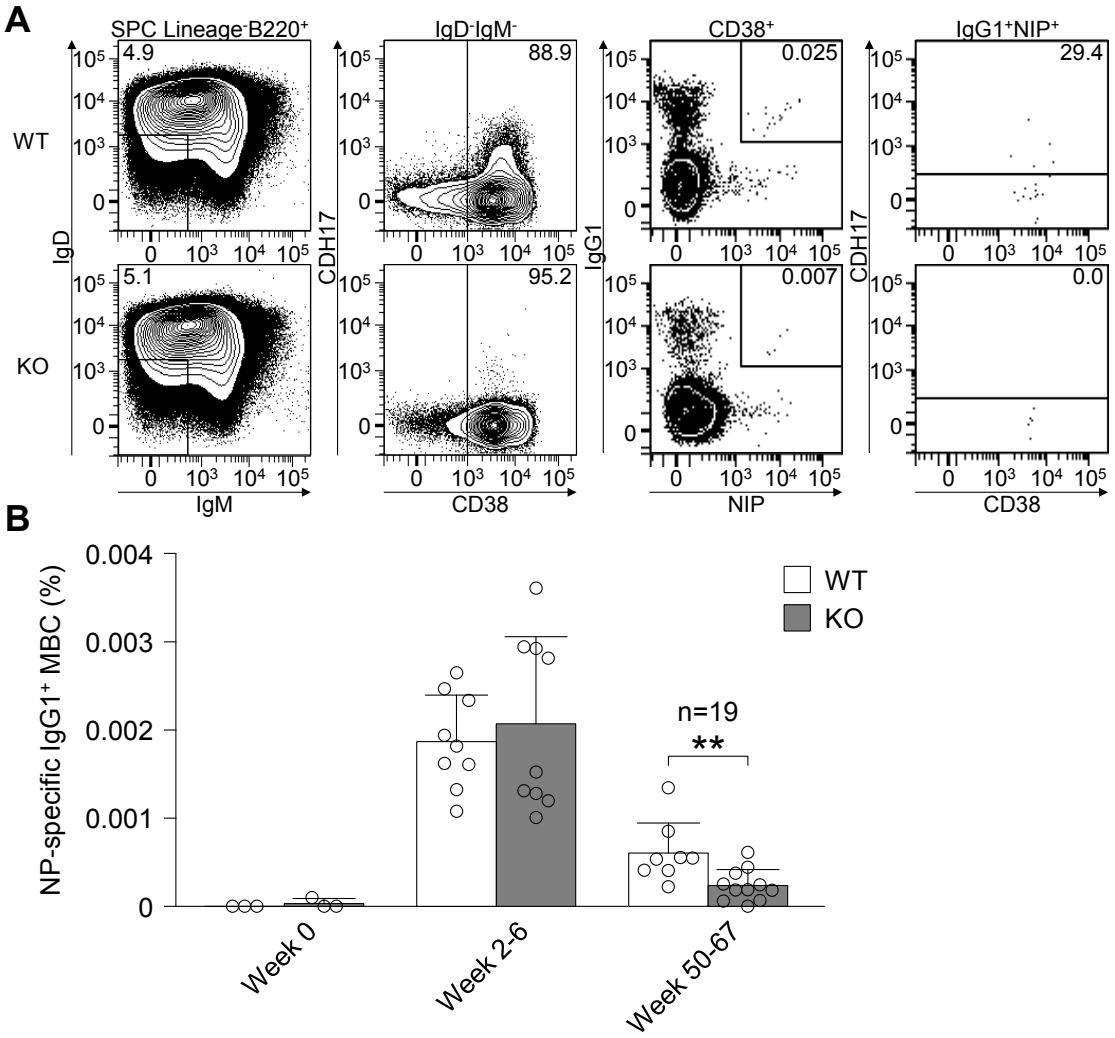

Figure 10. Long-term maintenance of antigen-specific MBCs is impaired in CDH17$^{-/-}$ mice.

(A) Flow cytometry analysis of antigen-specific IgG1^{+} MBCs (Lin^{-}B220^{+}IgD^{-}IgM^{-}CD38^{+}IgG1^{+}NIP^{+}) obtained from CDH17$^{-/-}$ (KO) mice and their WT littermates at 52 weeks after primary immunization with NP-CGG in alum. Numbers represent the percentage (%) of the indicated cell populations in the respective parental gates (shown on top of the panels). (B) Histogram showing the percentage of antigen-specific IgG1^{+} MBCs in their respective B220^{+} parental gate. The number of weeks post-immunization is shown for each bin. Each symbol represents an individual mouse (n=6 (Week 0); n=18 (Weeks 2–6); n=19 (Weeks 50–67); **P≤0.01 (Mann-Whitney U-test)).

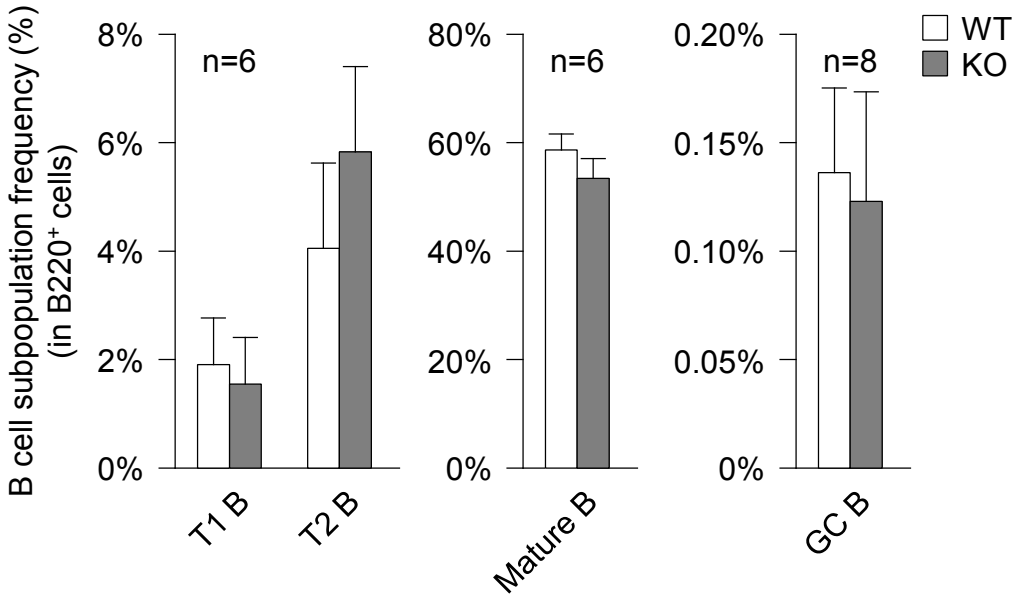

Figure 11. The percentage of MBC precursor cells is similar in WT and CDH17$^{-/-}$ mice.

Histogram showing the percentage of different splenic B cell populations (analyzed as described in the legend to Figure 2F) (n=2 (PCs); n=8 (GC B); n=6 (other)). *P≤0.05, **P≤0.01, ***P≤0.001 (Student's t-test)).

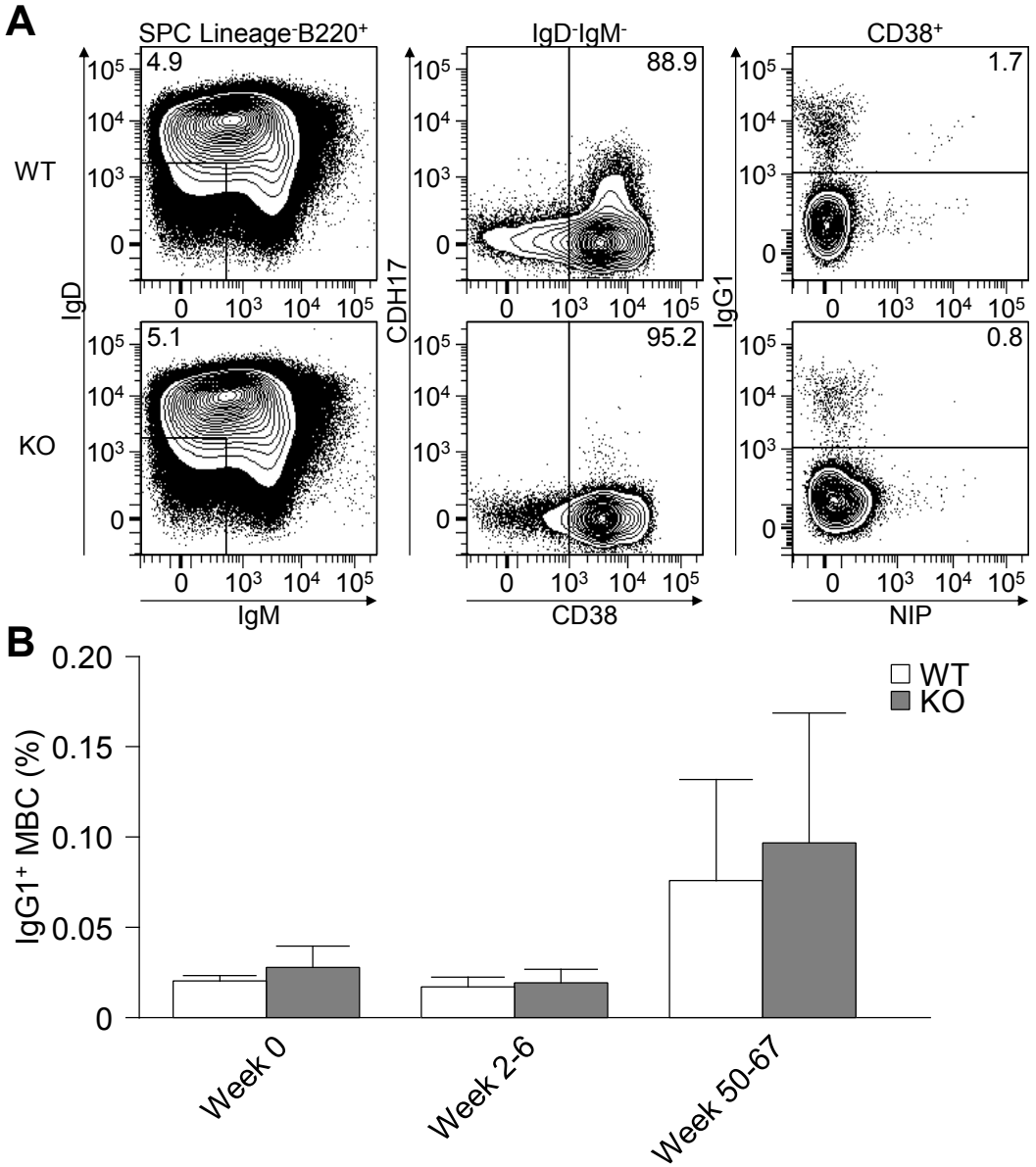

Figure 12. The percentage of total IgG1$^+$ MBCs is similar in WT and CDH17$^{-/-}$ mice.

(A) Flow cytometry analysis of IgG1$^+$ MBCs (Lin$^-$B220$^+$IgD$^-$IgM$^-$CD38$^+$IgG1$^+$) obtained from CDH17$^{-/-}$ (KO) mice and their WT littermates at 52 weeks after primary immunization with NP-CGG in alum. Numbers represent the percentage (%) of the indicated cell populations in the respective parental gates (shown on top of the panels). The same experiments described in Figure 10. (B) The percentage of IgG1$^+$ MBCs. The y-axis shows the percentage of IgG1$^+$ MBCs (Lin$^-$B220$^+$IgD$^-$IgM$^-$CD38$^+$IgG1$^+$) in the respective B220$^+$ parental gate. The number of weeks post-immunization is shown for each bin.

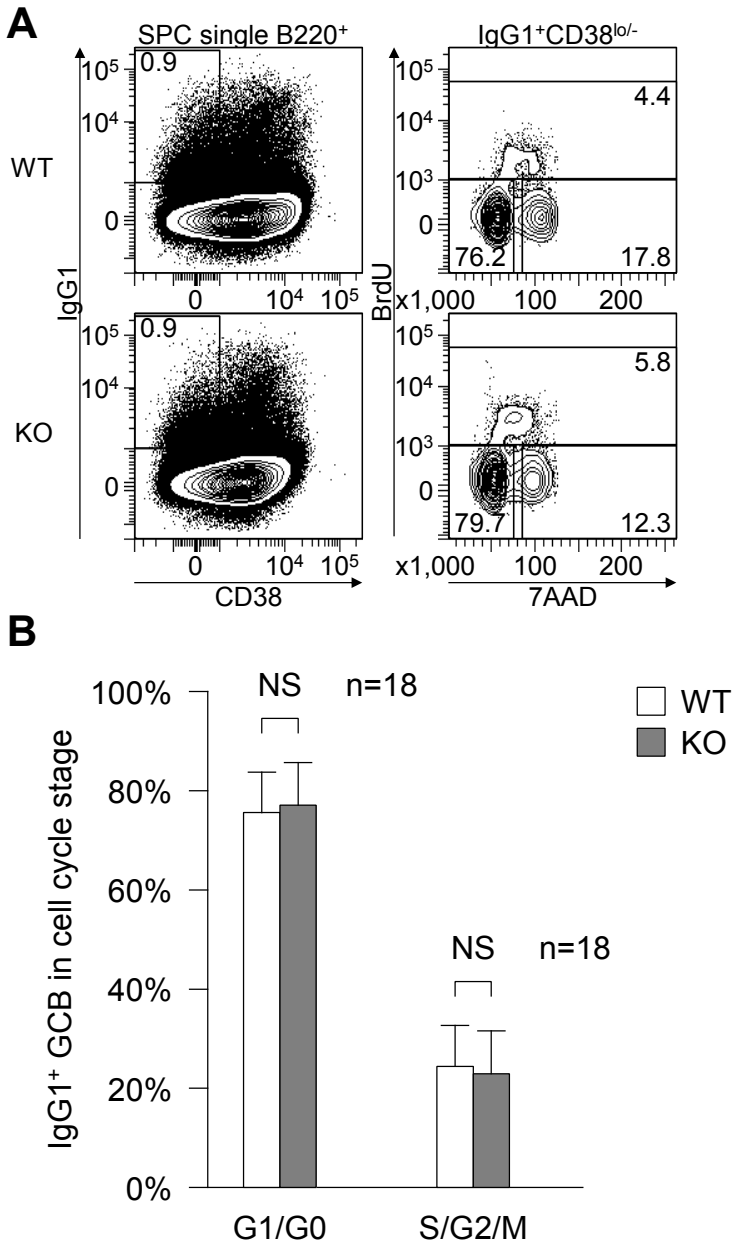

Figure 13. Cell cycle analysis of IgG1$^+$ GCB cells.

(A) Flow cytometry cell cycle analysis of IgG1$^+$ GCB cells (B220$^+$IgG1$^+$CD38$^{lo/-}$) from CDH17$^{-/-}$ (KO) mice and their WT littermates. Numbers indicate the percentage (%) of cells in their respective cell cycle gates (lower left, G0/G1 phase; top, S phase; lower right, G2/M phase). (B) Histogram showing the percentage of the GCB cell population in each indicated cell cycle stage (n=18; NS, not significant (P>0.05; Mann-Whitney U-test)).

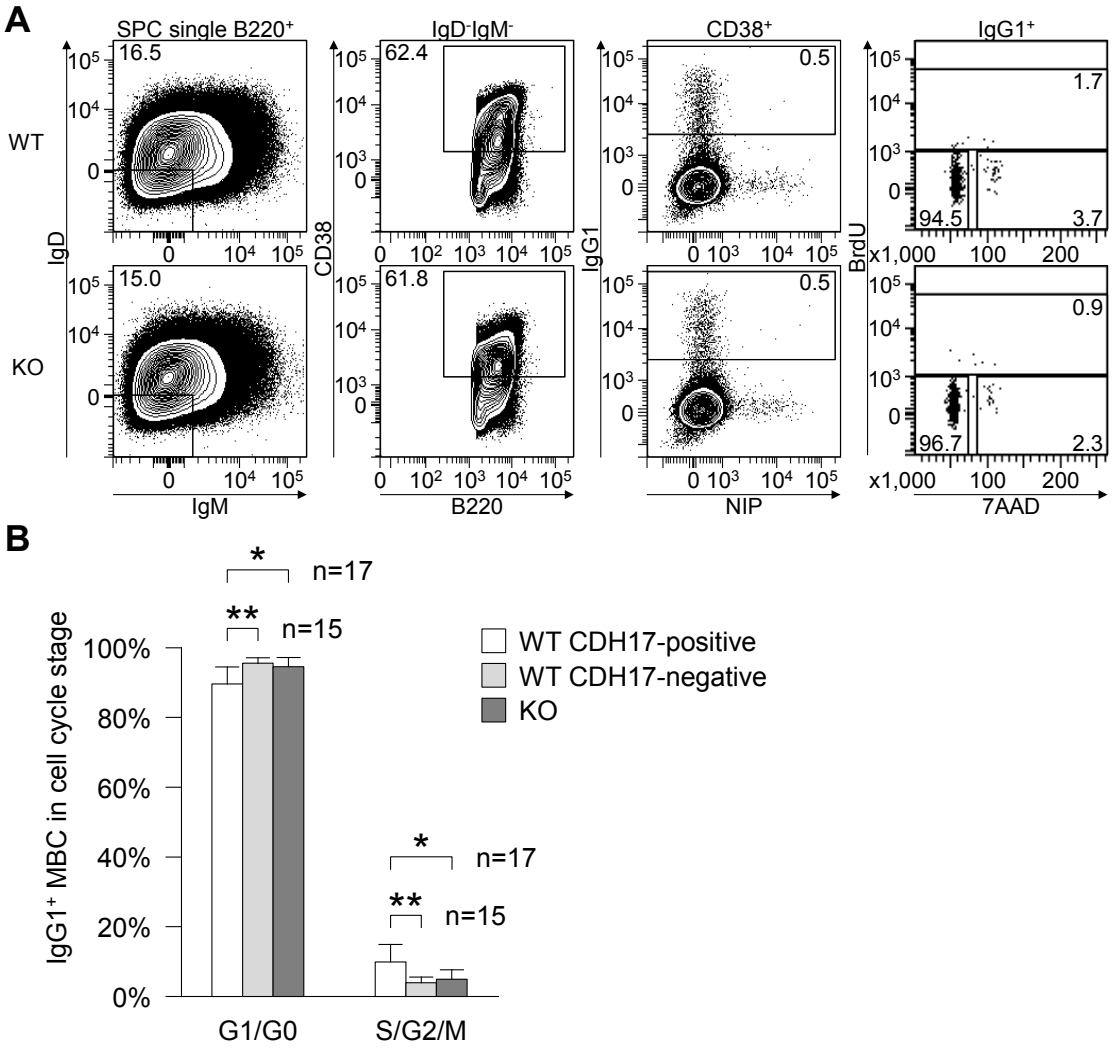

Figure 14. CDH17^{+} switched IgG1^{+} MBCs show increased cell cycle progression.

(A) Flow cytometry analysis of switched IgG1^{+} MBCs (B220^{+}IgD^{-}IgM^{-}CD38^{+}IgG1^{+}) from CDH17$^{-/-}$ (KO) mice and WT littermates. The numbers indicate the percentage of cells in the respective cell cycle gates as in Figure 13. (B) Histogram showing the percentage of switched IgG1^{+} MBCs at the indicated cell cycle stage (n=15–17; *P≤0.05, **P≤0.01 (Mann-Whitney U-test).

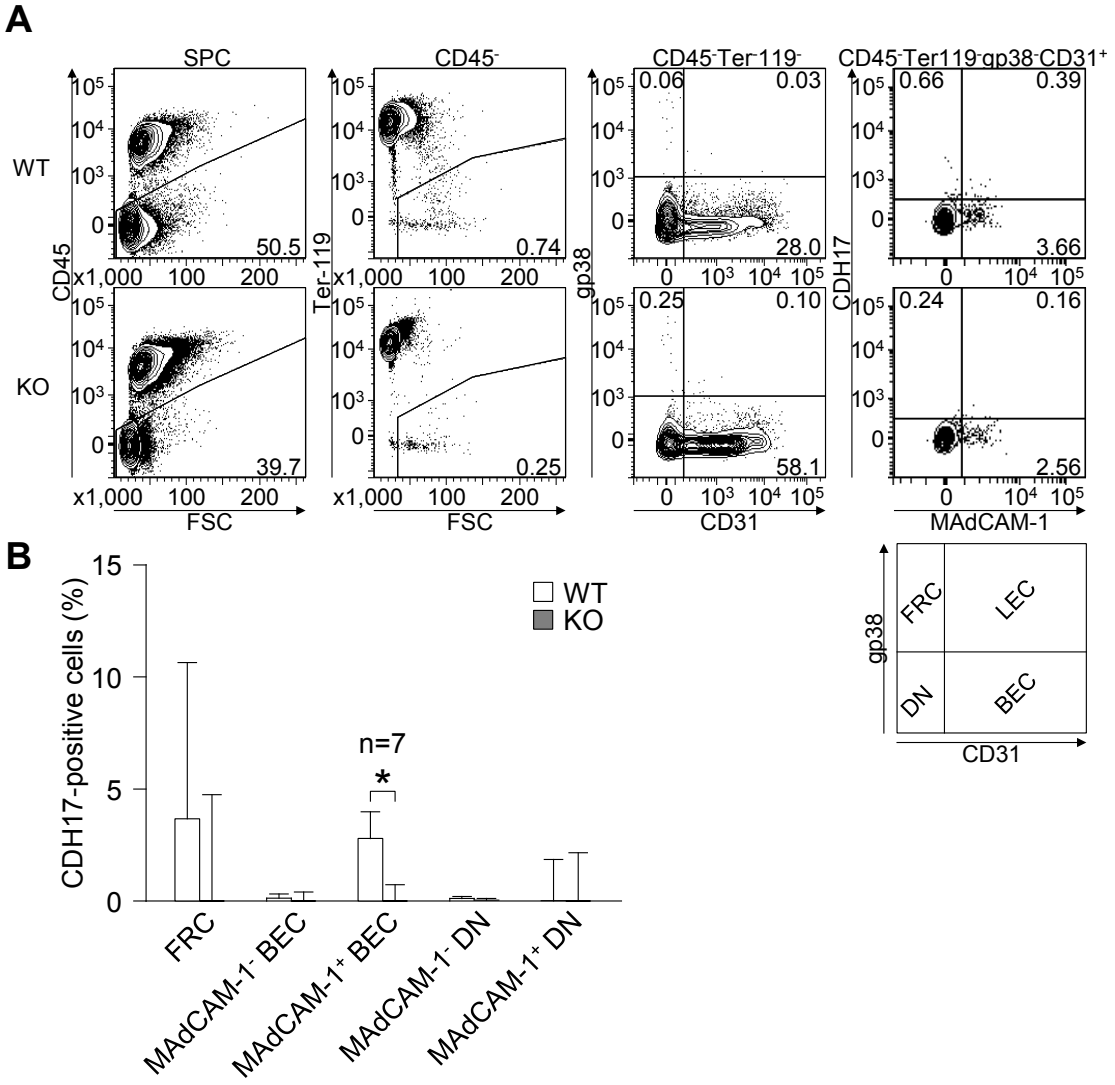

Figure 15. A fraction of BEC is CDH17^{+}.

(A) Spleens were treated with dispase and collagenase IV to obtain single stromal cells, and cell surface markers were analyzed by flow cytometry. Stromal cells were separated into four subpopulations: fibroblastic reticular cells (FRCs, gp38^{+}CD31^{-}), lymphatic endothelial cells (LECs, gp38^{+}CD31^{+}), blood endothelial cells (BECs, gp38^{-}CD31^{+}) and double-negative (DN) cells (far right panel). Each fraction was then tested for CDH17 expression. The numbers adjacent to the gates indicate the percentage (%) of the indicated cells within their respective parental gates (shown on top of each panel). (B) Histogram showing the percentage of CDH17^{+} stromal cells within the respective parental gates. The percentages were calculated by subtracting the values of CDH17$^{-/-}$ (KO) mice from those of WT mice (n=7 (MAdCAM-1^{+} BEC); n=8 (others)). *P≤0.05 (Student's t-test).

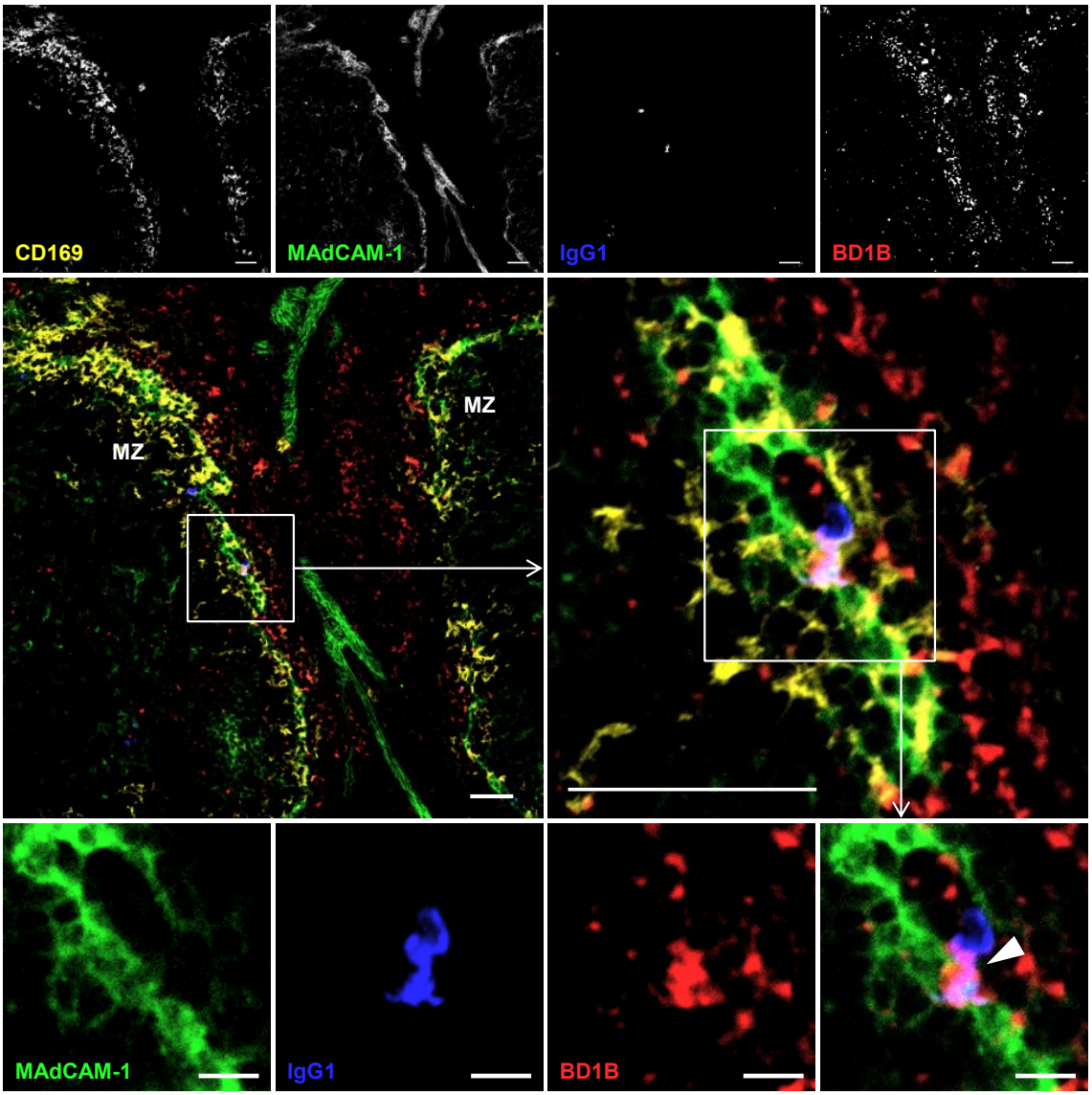

Figure 16. Microarchitecture of CDH17$^+$ stromal cells and IgG1$^+$ B cells in spleen.

Confocal microscopic image of WT mouse spleen stained with anti-CD169 (yellow), anti-MAdCAM-1 (green), anti-mouse IgG1 (blue), and anti-CDH17 (red, BD1B). The middle-right micrograph is an enlarged view of the boxed area shown in the middle-left micrograph. The bottom row of images shows each separate color channel and an expanded view of the merged image shown within the box in the middle-right panel. The white arrowhead shown in the bottom right image indicates an IgG1$^+$ cell that is adjacent to a CDH17$^+$ cell in the MZ sinus. Data are representative of three independent experiments. Scale bars, 50 μm (top and middle row of images) or 10 μm (bottom row).

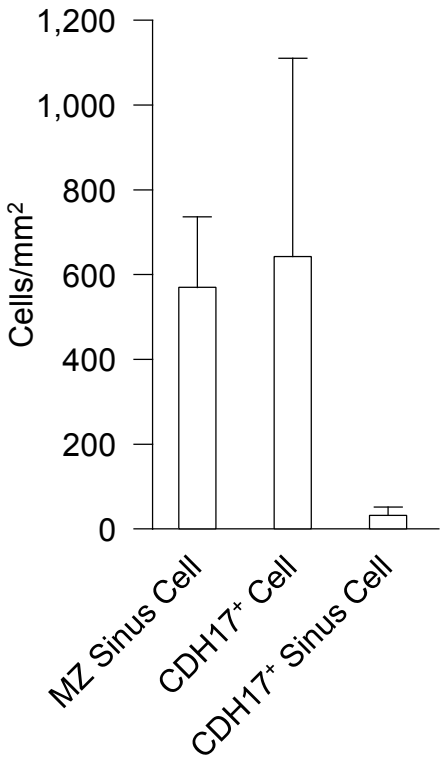

Figure 17. Quantification of CDH17$^+$ MZ sinus cells.

Histogram shows the number of MZ sinus (MAdCAM-1$^+$) cells, CDH17$^+$ cells, and CDH17$^+$ MZ sinus cells (CDH17$^+$MAdCAM-1$^+$) in the spleen of WT mice. Cell numbers were counted in six histological sections of WT spleen. The mean and standard deviation are plotted.

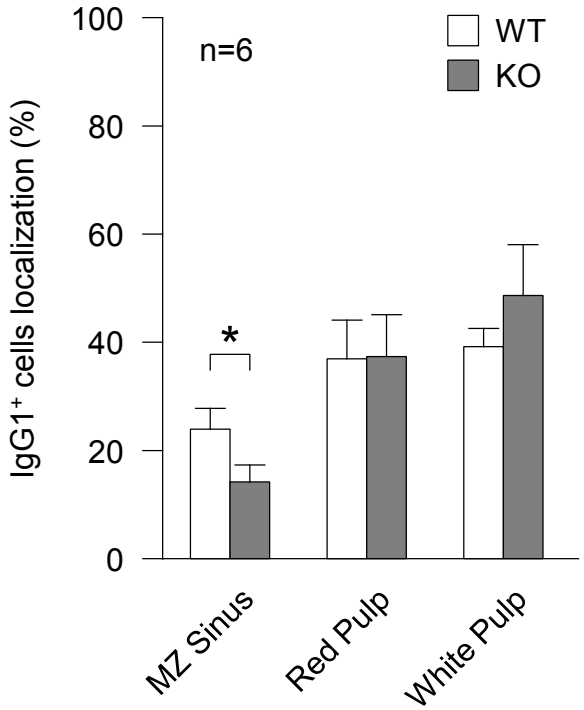

Figure 18. The localization of IgG1$^+$ cells in spleen.

Histogram showing the localization of IgG1$^+$ cells in the MZ, red pulp, and white pulp in WT and CDH17$^{-/-}$ (KO) mice. Values are expressed as the percentage of IgG1$^+$ cells localized within each sub-region of the spleen. Data were obtained by confocal microscopy as in Figure 16 (n=6; *P≤0.05 (Student's t-test)).

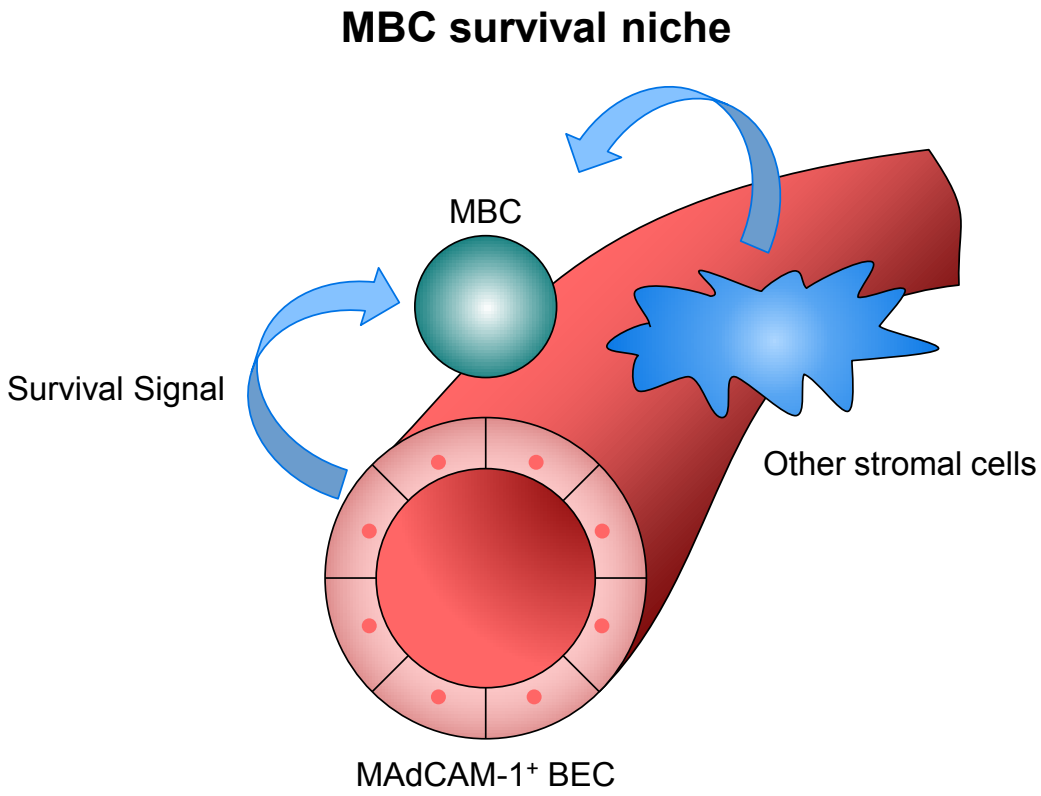

Figure 19. A model of the MBC survival niche.

In spleen, a fraction of MAdCAM-1^+ BEC expressed CDH17 lining the marginal sinuses. MBCs adhere with the CDH17^+MAdCAM-1^+ BEC by the homotypic adhesion of CDH17. Then MBC was anchored on the MAdCAM-1^+ BEC and receive survival signals. By this way, it enables the long-term maintenance of MBC.

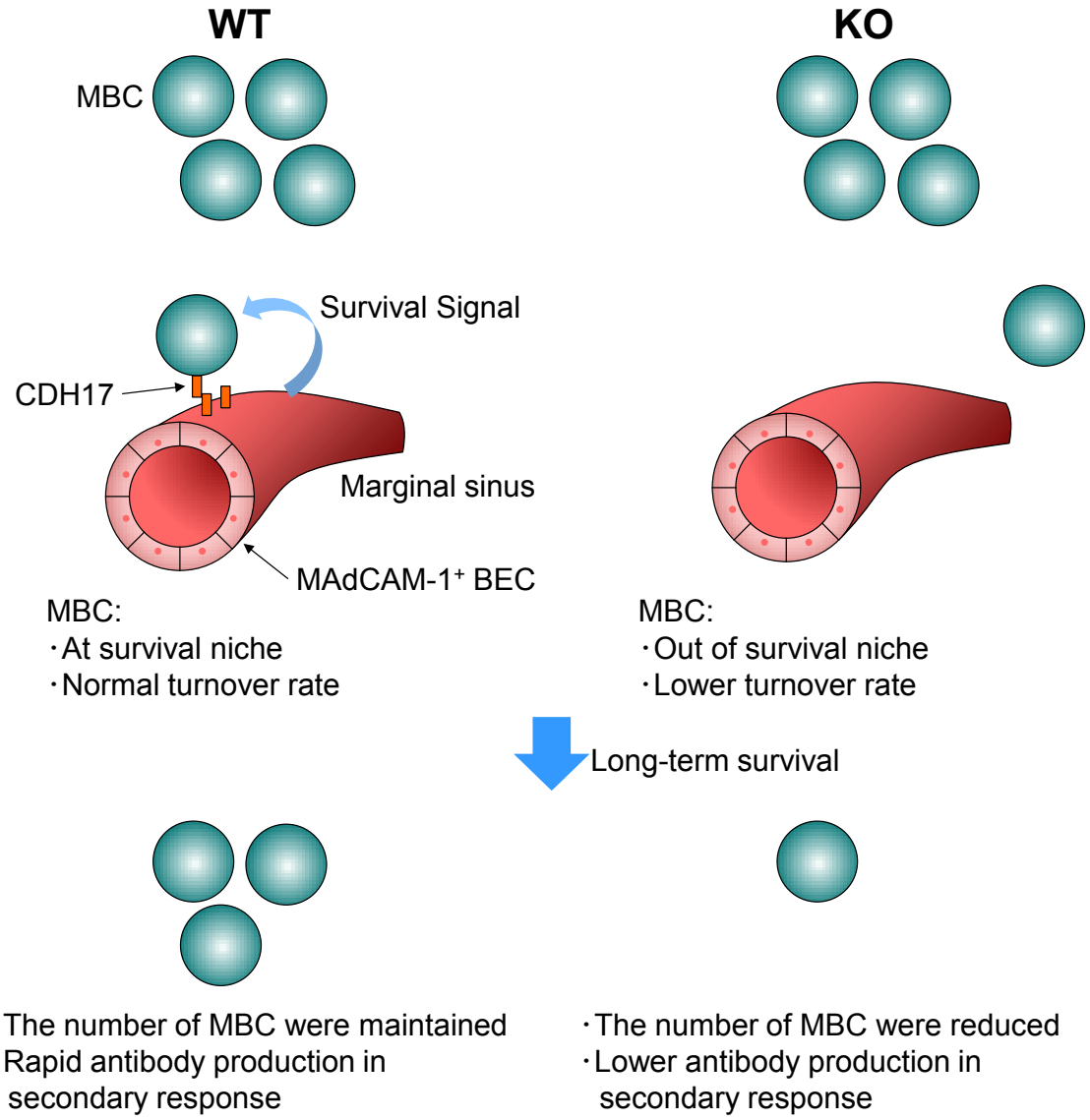

Figure 20. A schematic model of long-term MBC maintenance.

MBCs in WT mice can be anchored by CDH17-positive MAdCAM-1-positive BEC at marginal sinus via the homotypic adhesion of CDH17. Then the MBC can receive survival signal from stromal cells and shows normal turnover rate. In contrast, MBCs in CDH17$^{-/-}$ (KO) mice cannot be localized at the niche, so that it cannot receive survival signal and shows lower turnover rate. Then, the long-term maintenance of MBC and the secondary antibody response are impaired in CDH17$^{-/-}$ mice (see text for further description).